Multiquark states at LHCb

Results and prospects

A. Augusto Alves Jr.

University of Cincinnati
aalvesju@cern.ch

Experimental Particle and Astro-Particle Physics Seminar,
29 Febuary 2016, Zurich

Outline

1. The LHC accelerator and its detectors
2. Exotic states
3. Results on $P(4380)^+_c$
4. Results on $Z(4430)^+$
5. $\mathrm{X}(3872)$ quantum numbers and $\rho \mathrm{J}/\psi$
6. Light meson spectroscopy
7. Conclusions

The LHC accelerator and its detectors

The LHC is designed to collide two high luminosity and high energy beams of protons or heavy ions.

- Two general purpose high luminosity experiments: CMS and ATLAS
- One low luminosity experiment, dedicated to flavour physics experiment: LHCb
- Heavy-ion experiment: ALICE

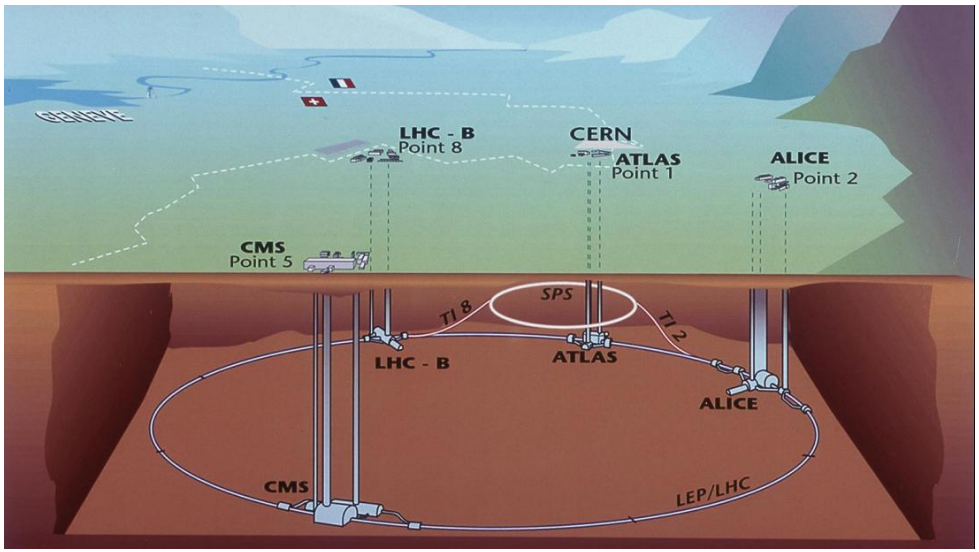

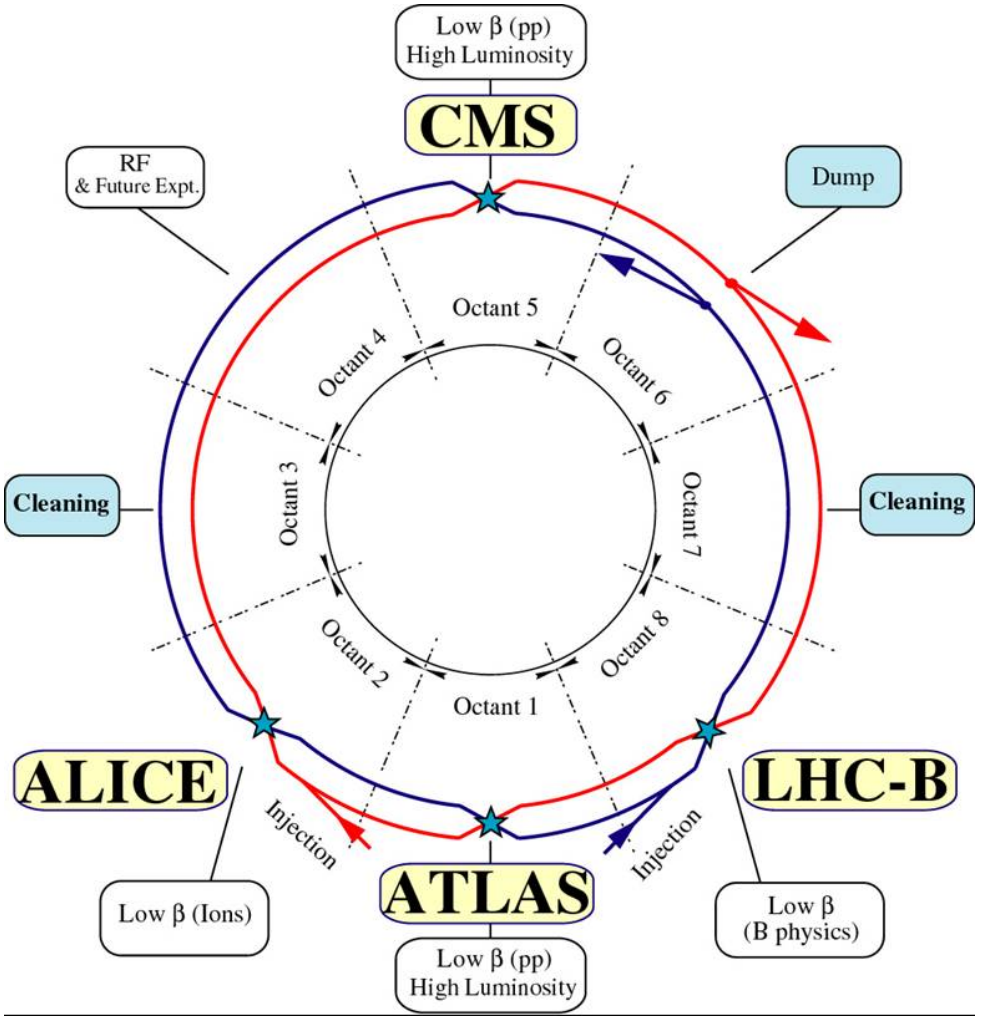

The LHC environment

During most of 2012 run, LHC collided protons at 8 TeV with an average instantaneous luminosity of $4 \times 10^{32} cm^{-2} s^{-1}$ (LHCb) and 20 MHz of bunch crossing.

- Inelastic cross section $\sim 60\,\mathrm{mb}$
- $\sigma(\mathrm{pp} \to \mathrm{b\bar{b}}X) = (284 \pm 20(\mathrm{stat}) \pm 49(\mathrm{syst}))\ \mu\mathrm{b}$ [PLB 694, 209]
- $\Longrightarrow$ $\sim 10^6$ $\mathrm{B\bar{B}}$ produced per second
- $\sigma(\mathrm{pp} \to c\bar{c}X)$ is about 20 times higher. [Nucl.Phys. B871 (2013) 1-20]

At the LHC energy, the $\mathrm{b\bar{b}}$ pairs are produced preferentially at forward (backward) directions.

- 4π acceptance design is not optimal for flavour physics.
- Optimal solution is a forward detector: LHCb

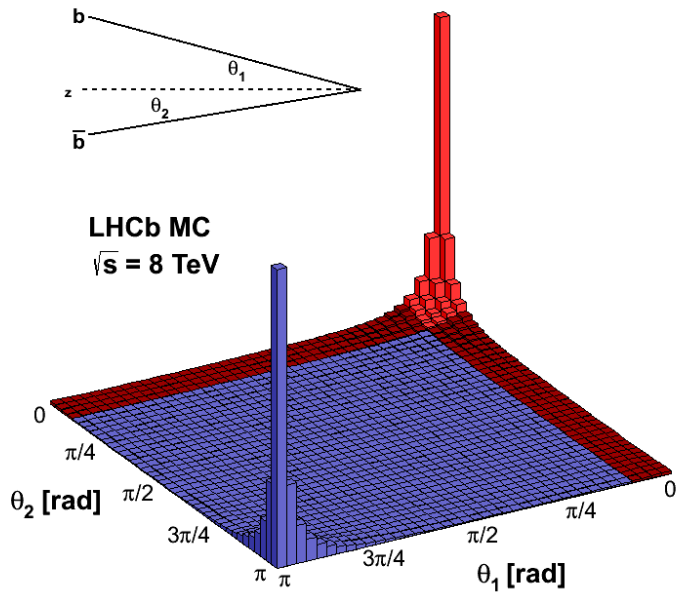

The LHCb detector

LHCb experiment was designed to perform high precision flavour physics measurements at the LHC.

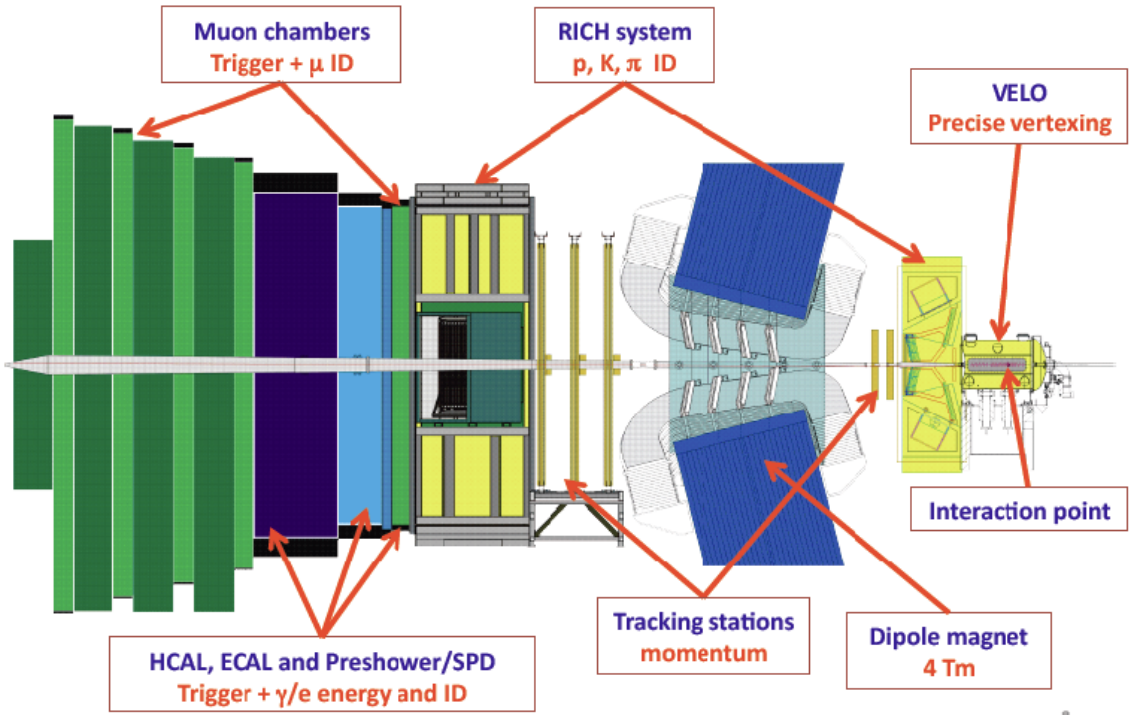

- **Single-arm design.** Covering the range $2 < \eta < 5$, LHCb can exploit the dominant heavy flavour production mechanism at the LHC and detects $\sim$ 40% of the $\mathrm{b\bar{b}}$ produced in forward region.
- **Good particle identification.** Excellent muon identification and good separation of π, K and p over (2 - 100) GeV.

- **Good vertexing and tracking.** Precise primary and secondary vertex reconstruction. Excellent momentum, IP and proper time resolution.
- **Dataset.** $1 + 2$ fb^{-1} acquired in 2011 + 2012 runs

Quarkonia status

In QCD-motivated models, quarkonia states are basically described as $q\bar{q}$ pairs bound by a short-distance potential approximately Coulombic (single-gluon exchange) plus a linearly increasing confining potential at large separations.

- All charmonium states below the $D\bar{D}$ mass threshold have been observed.
- Charmonium states above the $D\bar{D}$ or $D\bar{D}^*$ mass threshold can decay into $D\bar{D}$ and $D\bar{D}^*$ final states.
- Many predicted states still not observed.
- Similar situation in the Beauty sector.

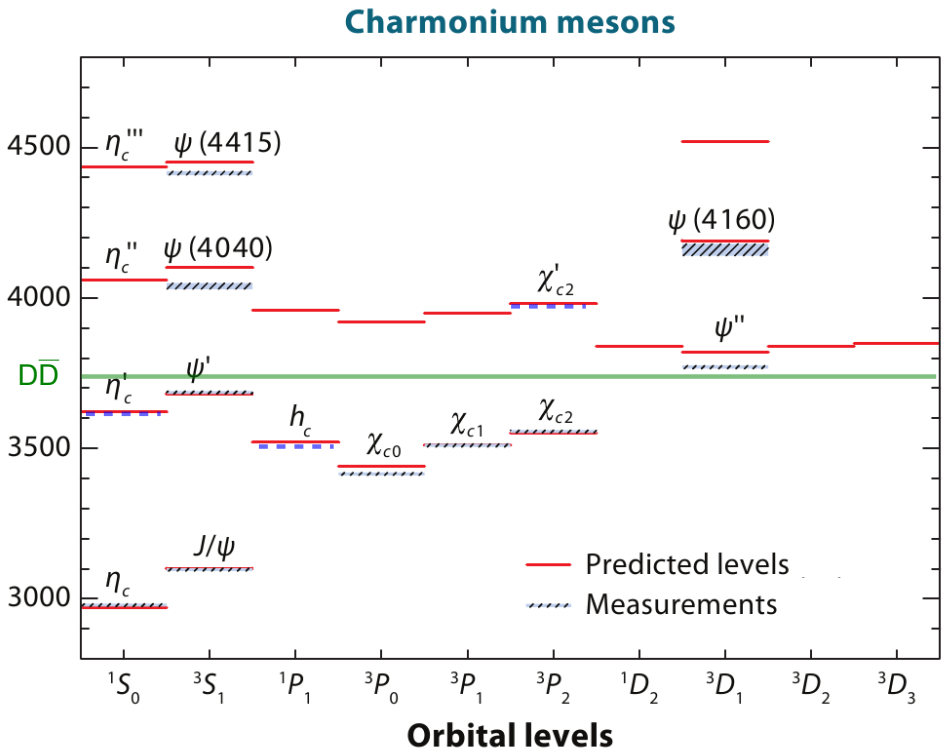

Figure from [Annu.Rev.Nucl. Part. Sci. 2008. 58:51–73]

XYZ states

Many new states have been observed at c-, b-factories and Tevatron

- Masses lying on the limits of the quarkonia spectrum
- Observed many different production mechanisms: ISR, e^+e^-, $\gamma\gamma$ and B decays.
- The measured masses do not correspond to the predicted values for conventional quarkonia.
- The properties do not fit very well to the quarkonia picture.

Many theoretical interpretations in discussion:

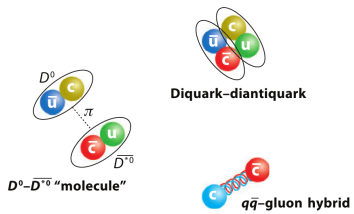

- conventional quarkonia;
- multiquark states;
- meson-molecules;
- hybrid mesons;
- threshold effects;

The table should be updated to include some new states: $P(4380)^+_c$, $P(4450)^+_c$ ...

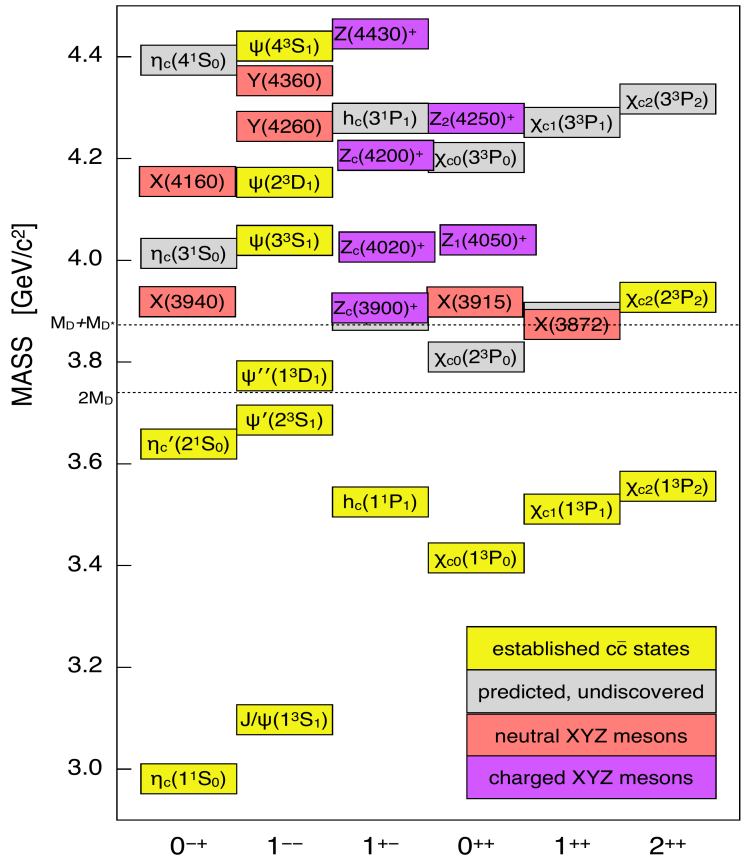

[PoS Bormio 050(2015) arXiv:1511.01589]

XYZ states

Many new states have been observed at Charm, B-factories and Tevatron

- Masses lying on the limits of the quarkonia spectrum
- Observed many different production mechanisms: ISR, e^+e^-, $\gamma\gamma$ and B decays.
- The measured masses do not correspond to the predicted values for conventional quarkonia.
- The properties do not fit very well to the quarkonia picture.

Many theoretical interpretations in discussion:

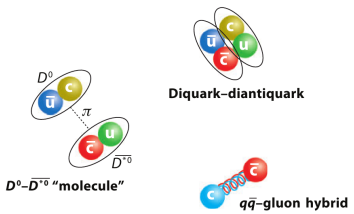

- conventional quarkonia;
- multiquark states;
- meson-molecules;
- hybrid mesons;
- threshold effects;

The table should be updated to include some new states: $P(4380)_c^+$, $P(4450)_c^+$ ...

State	M (MeV)	Γ (MeV)	J^{PC}	Process (decay mode)
$X(3872)$	3871.68 ± 0.17	<1.2	1^{++}	$B\to K+(J/\psi\pi^+\pi^-)$
				$p\bar{p}\to(J/\psi\pi^+\pi^-)+\ldots$
				$B\to K+(J/\psi\pi^+\pi^-\pi^0)$
				$B\to K+(D^0\bar{D}^0\pi^0)$
				$B\to K+(J/\psi\gamma)$
				$B\to K+(\psi'\gamma)$
				$pp\to(J/\psi\pi^+\pi^-)+\ldots$
$X(3915)$	3917.4 ± 2.7	28^{+10}_{-9}	0^{++}	$B\to K+(J/\psi\omega)$
				$e^+e^-\to e^+e^-+(J/\psi\omega)$
$X(3940)$	3942^{+9}_{-8}	37^{+27}_{-17}	$0(?)^{-(?)+}$	$e^+e^-\to J/\psi+(D^*\bar{D})$
				$e^+e^-\to J/\psi+(\ldots)$
				$e^+e^-\to\gamma+(D\bar{D})$
				$e^+e^-\to\gamma+(J/\psi\pi^+\pi^-)$
				$B\to K+(J/\psi\phi)$
				$e^+e^-\to J/\psi+(D^*\bar{D})$
				$e^+e^-\to\gamma+(J/\psi\pi^+\pi^-)$
				$e^+e^-\to(J/\psi\pi^+\pi^-)$
				$e^+e^-\to(J/\psi\pi^0\pi^0)$
$Y(4360)$	4361 ± 13	74 ± 18	1^{--}	$e^+e^-\to\gamma+(\psi'\pi^+\pi^-)$
$X(4630)$	4634^{+9}_{-11}	92^{+41}_{-32}	1^{--}	$e^+e^-\to\gamma(\Lambda_c^+\Lambda_c^-)$
$Y(4660)$	4664 ± 12	48 ± 15	1^{--}	$e^+e^-\to\gamma+(\psi'\pi^+\pi^-)$
$Z_c^+(3900)$	3890 ± 3	33 ± 10	1^{+-}	$Y(4260)\to\pi^-+(J/\psi\pi^+)$
				$Y(4260)\to\pi^-+(D\bar{D}^*)^+$
$Z_c^+(4020)$	4024 ± 2	10 ± 3	$1(?)^{+(?)-}$	$Y(4260)\to\pi^-+(h_c\pi^+)$
				$Y(4260)\to\pi^-+(D^*\bar{D}^*)^+$
$Z_c^0(4020)$	4024 ± 4	10 ± 3	$1(?)^{+(?)-}$	$Y(4260)\to\pi^0+(h_c\pi^0)$
$Z_1^+(4050)$	4051^{+24}_{-43}	82^{+51}_{-55}	$?^{?+}$	$B\to K+(\chi_{c1}\pi^+)$
$Z^+(4200)$	4196^{+35}_{-32}	370^{+99}_{-149}	1^{+-}	$B\to K+(J/\psi\pi^+)$
$Z_2^+(4250)$	4248^{+185}_{-45}	177^{+321}_{-72}	$?^{?+}$	$B\to K+(\chi_{c1}\pi^+)$
$Z^+(4430)$	4477 ± 20	181 ± 31	1^{+-}	$B\to K+(\psi'\pi^+)$
				$B\to K+(J\psi\pi^+)$
$Y_b(10890)$	10888.4 ± 3.0	$30.7^{+8.9}_{-7.7}$	1^{--}	$e^+e^-\to(\Upsilon(nS)\pi^+\pi^-)$
$Z_b^+(10610)$	10607.2 ± 2.0	18.4 ± 2.4	1^{+-}	$\Upsilon(5S)\to\pi^-+(\Upsilon(1,2,3S)\pi^+)$
				$\Upsilon(5S)\to\pi^-+(h_b(1,2P)\pi^+)$
				$\Upsilon(5S)\to\pi^-+(B\bar{B}^*)^+$
$Z_b^0(10610)$	10609 ± 6		1^{+-}	$\Upsilon(5S)\to\pi^0+(\Upsilon(1,2,3S)\pi^0)$
$Z_b^+(10650)$	10652.2 ± 1.5	11.5 ± 2.2	1^{+-}	$\Upsilon(5S)\to\pi^-+(\Upsilon(1,2,3S)\pi^+)$
				$\Upsilon(5S)\to\pi^-+(h_b(1,2P)\pi^+)$
				$\Upsilon(5S)\to\pi^-+(B^*\bar{B}^*)^+$

[PoS Bormio 050(2015) arXiv:1511.01589]

$\Lambda_b^0 \to K^- \bar{p} J/\psi$

Phys. Rev. Lett. 115 (2015) 072001

- Sample with >26.000 $\Lambda_b^0 \to K^- \bar{p} J/\psi$ signal candidates,
- Analysis: six-dimensional amplitude fit (invariant masses, helicity and decay planes angles).
- Background from sidebands. Estimated 5.4% of combinatorial background in the signal region.
- Six-dimensional efficiency calculated using complete simulation of the detector

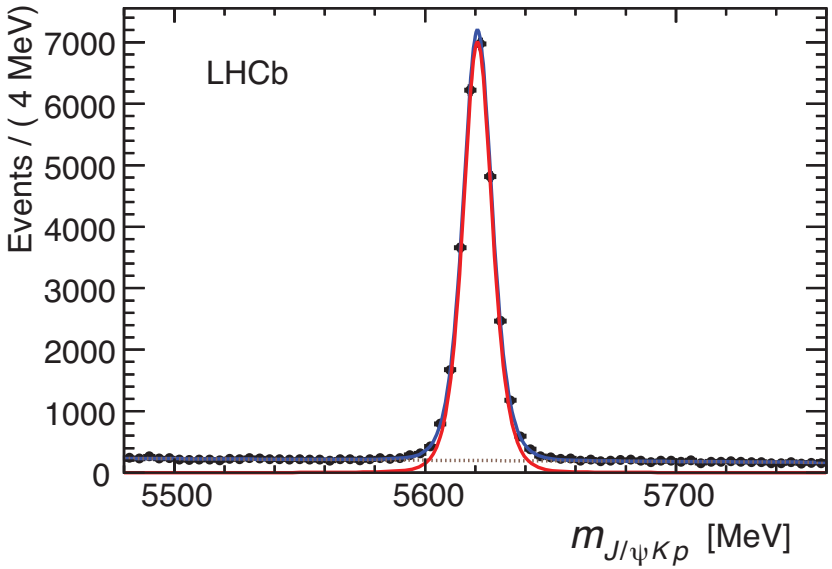

background subtracted Dalitz plot

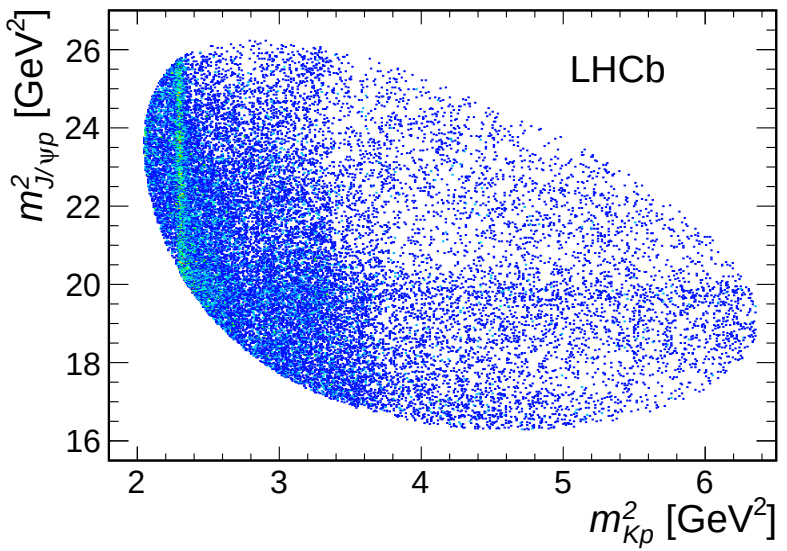

$\Lambda_b^0 \to K^- p J/\psi$

Some analysis details

- Two parametizations: $\Lambda_b^0 \to K^- (P_c^+ \to p J/\psi)$ and $\Lambda_b^0 \to J/\psi (\Lambda^* \to p K^-)$, with $J/\psi \to \mu^+ \mu^-$

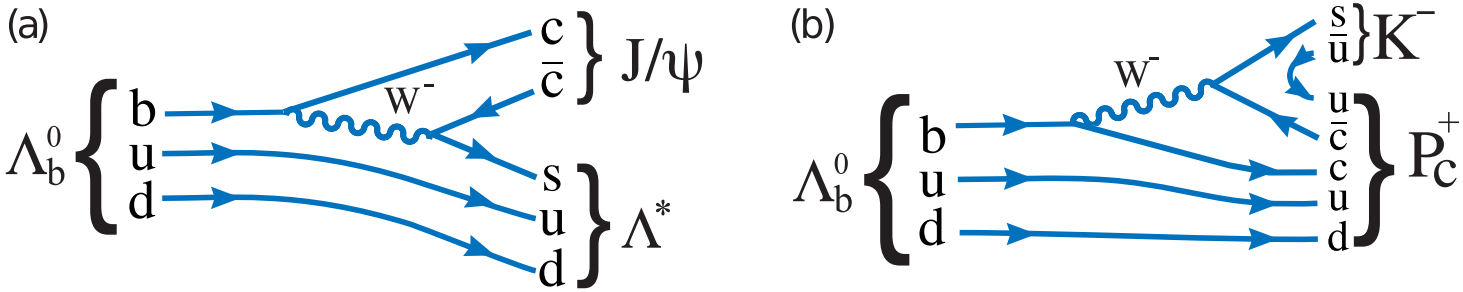

- Six-dimensional amplitude fit. Resonance invariant mass, three helicities angles, and two differences between decay planes.

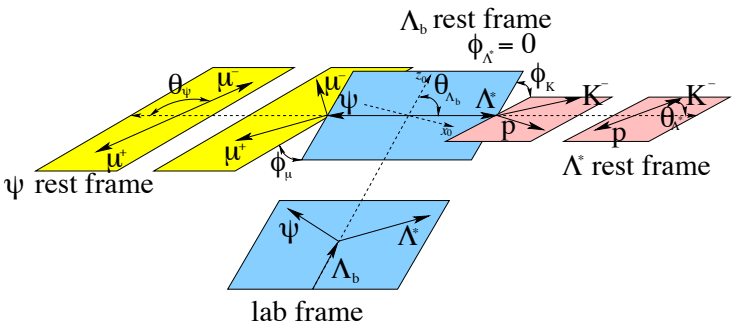

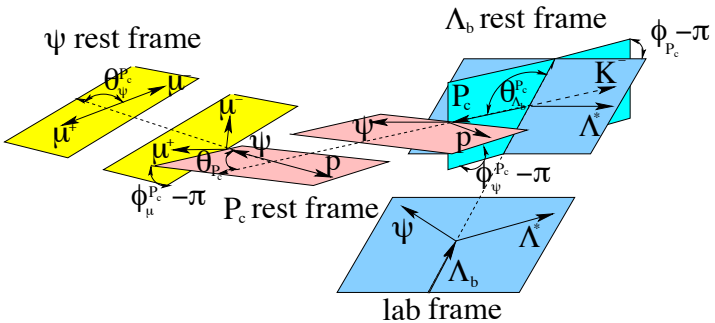

- Lorentz transformations relates the two helicity representantions.
- Resonances described by Breit-Wigner.
- Angular distribution calculated using helicity formalism.

$\Lambda_b^0 \to K^- p J/\psi$

Fit results without pentaquark states

- Fit including only Λ^* resonances, allowing all possible known states (Extended model)
- The masses and widths of the Λ^* states are fixed to their PDG values
- The m_{Kp} distribution is reasonably well fitted
- The peaking structure in $m_{J/\psi p}$ is not described

State	J^P	M_0 (MeV)	Γ_0 (MeV)	# Reduced	# Extended
$\Lambda(1405)$	$1/2^-$	$1405.1^{+1.3}_{-1.0}$	50.5 ± 2.0	3	4
$\Lambda(1520)$	$3/2^-$	1519.5 ± 1.0	15.6 ± 1.0	5	6
$\Lambda(1600)$	$1/2^+$	1600	150	3	4
$\Lambda(1670)$	$1/2^-$	1670	35	3	4
$\Lambda(1690)$	$3/2^-$	1690	60	5	6
$\Lambda(1800)$	$1/2^-$	1800	300	4	4
$\Lambda(1810)$	$1/2^+$	1810	150	3	4
$\Lambda(1820)$	$5/2^+$	1820	80	1	6
$\Lambda(1830)$	$5/2^-$	1830	95	1	6
$\Lambda(1890)$	$3/2^+$	1890	100	3	6
$\Lambda(2100)$	$7/2^-$	2100	200	1	6
$\Lambda(2110)$	$5/2^+$	2110	200	1	6
$\Lambda(2350)$	$9/2^+$	2350	150	0	6
$\Lambda(2585)$	?	$\approx$2585	200	0	6

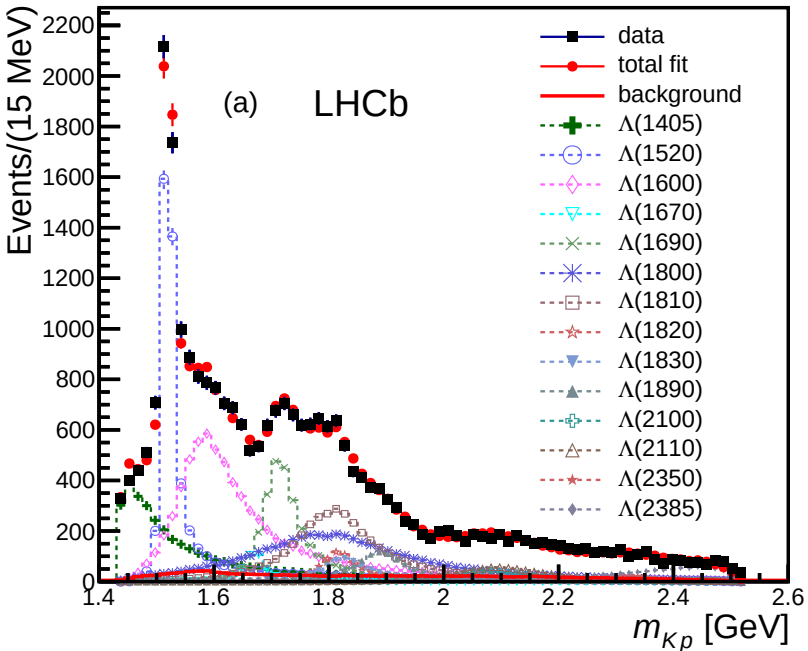

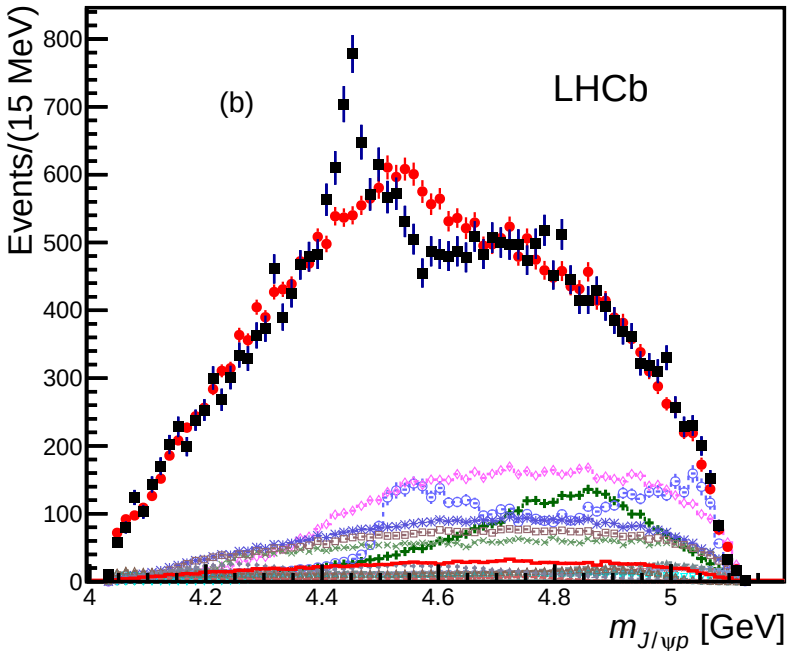

$\Lambda_b^0 \to K^- p J/\psi$

Fit results with pentaquark states

- Fit including just well motivated Λ^* resonances (Reduced model).
- Two P_c^+ states necessary to achieve acceptable fit quality.
- $P(4380)_c^+$ with $M = 4380 \pm 8 \pm 29\,\mathrm{MeV}/c^2$ and $\Gamma = 205 \pm 18 \pm 86\,\mathrm{MeV}/c^2$ $J^P = 3/2^-$, fit fraction of $(8.4 \pm 0.7 \pm 4.2)\%$ and significance of 9σ
- $P(4450)_c^+$ with $M = 4449.8 \pm 1.7 \pm 2.5\,\mathrm{MeV}/c^2$ and $\Gamma = 39 \pm 5 \pm 19\,\mathrm{MeV}/c^2$ $J^P = 5/2^+$, fit fraction $(4.1 \pm 0.5 \pm 1.1)\%$ and significance of 12σ
- The mass resolution is approximately $2.5\,\mathrm{MeV}/c^2$ and combined significance 15σ
- Systematic uncertainties: see table in the backup slides.

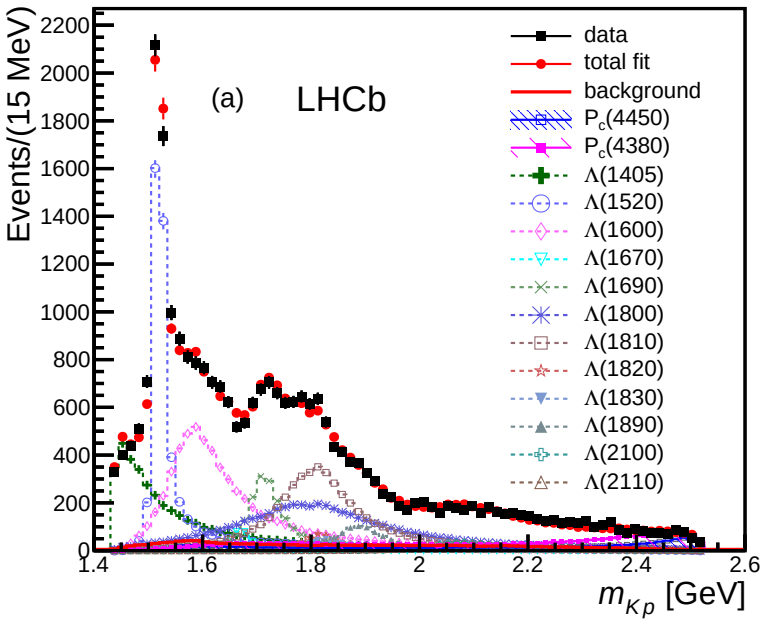

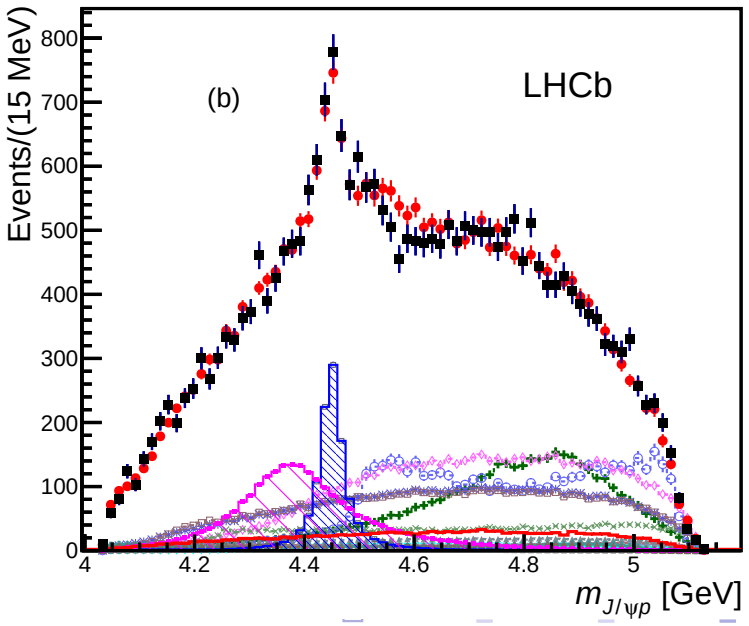

- $P(4450)_c^+$ amplitude is now described by 6 independent complex numbers instead of a Breit-Wigner
- Six equidistant points in the range $\pm\Gamma_0 = 39\,\mathrm{MeV}/c^2$ around $M_0 = 4449.8\,\mathrm{MeV}/c^2$ (from the default fit)
- Observe a fast change of phase crossing maximum of magnitude. Expected behavior for a resonance.
- Same test on $P(4380)_c^+$ leads to inconclusive results

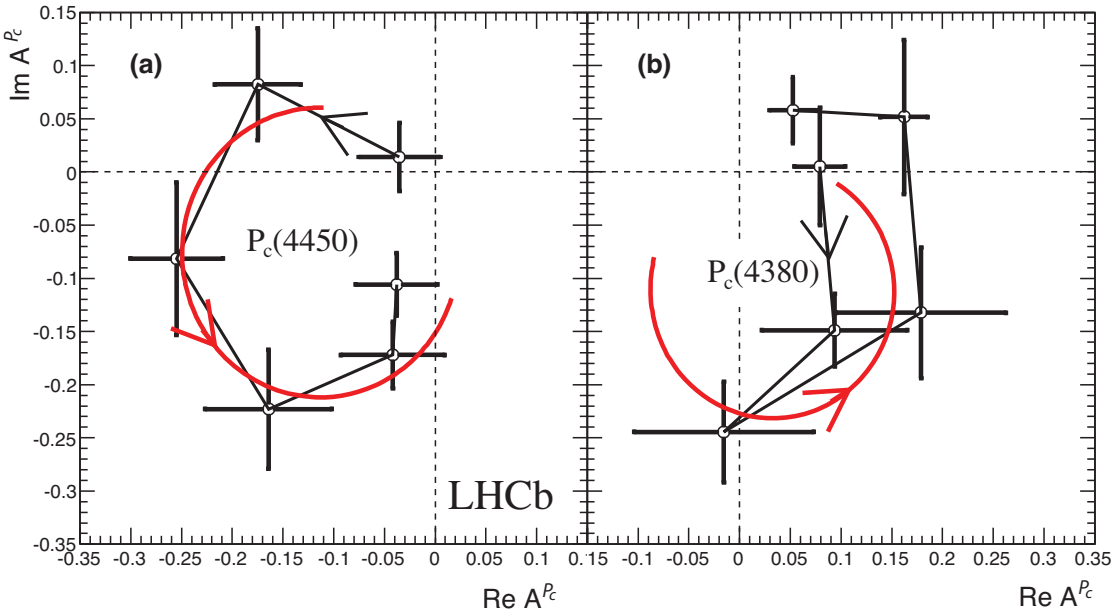

$Z(4430)^+$

- Charged charmonium like state reported by Belle in $B^0 \to \psi(2S)K^+\pi^-$ decays [Phys.Rev.D88:074026]
- Searched and not confirmed or excluded by BaBar [Phys.Rev.D79:112001]
- Can not be explained as conventional meson.
- Minimum quark content: $c\bar{c}u\bar{d}$
- No corresponding structure observed in $B^0 \to J/\psi K^+\pi^-$

$Z(4430)^+$ at Belle. K^{*0} and $K_2^*(1432)$ vetoed.

With $Z(4430)^+$ and No $Z(4430)^+$

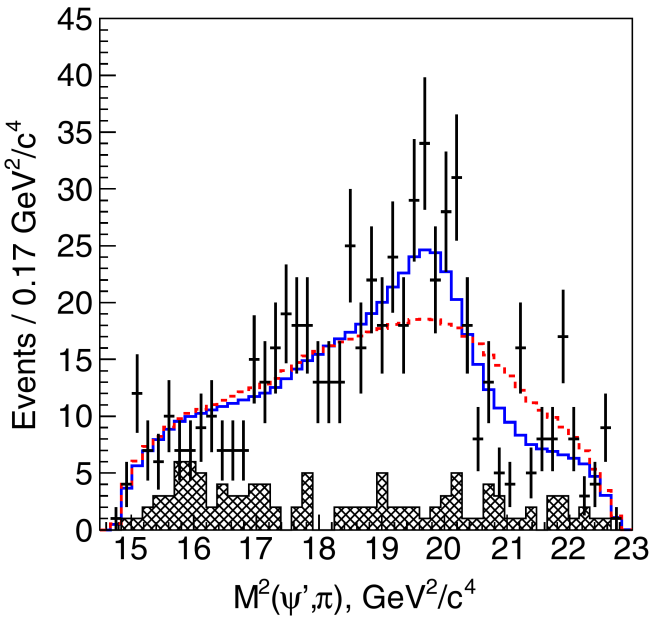

$Z(4430)^+$ at BaBar. Legendre polynomials approach.

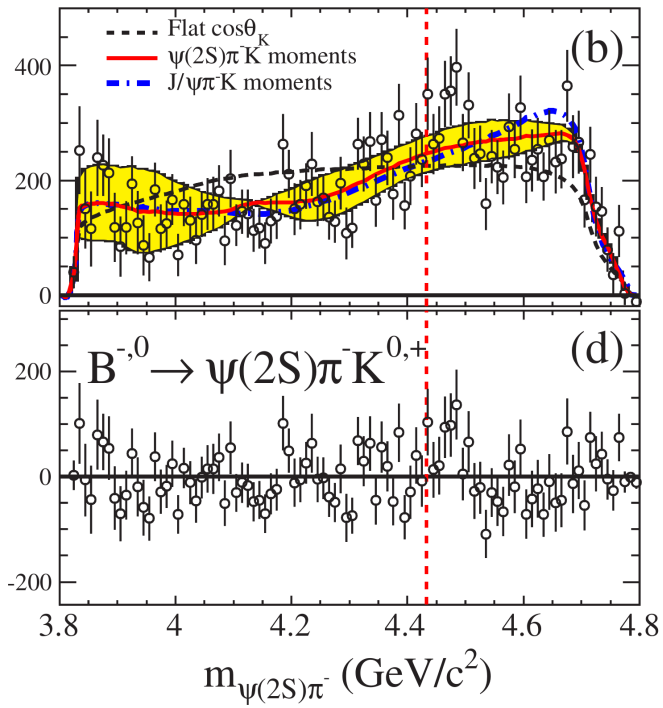

Confirmation of $Z(4430)^+$ at LHCb

Phys.Rev.Lett.112, 222002 (2014)

- Sample with >25.000 $B^0 \to K^+\pi^-\psi(2S)$ signal candidates,
- Analysis performed using two different approaches:
  - Model dependent. Four-dimensional amplitude fit (invariant masses, helicity and decay planes angles).
  - Model independent. An analysis based on the Legendre polynomial moments extracted from the $K\pi$ system
- Background from sidebands. Estimated 4% of combinatorial background in the signal region.
- Four-dimensional efficiency calculated using complete simulation of the detector

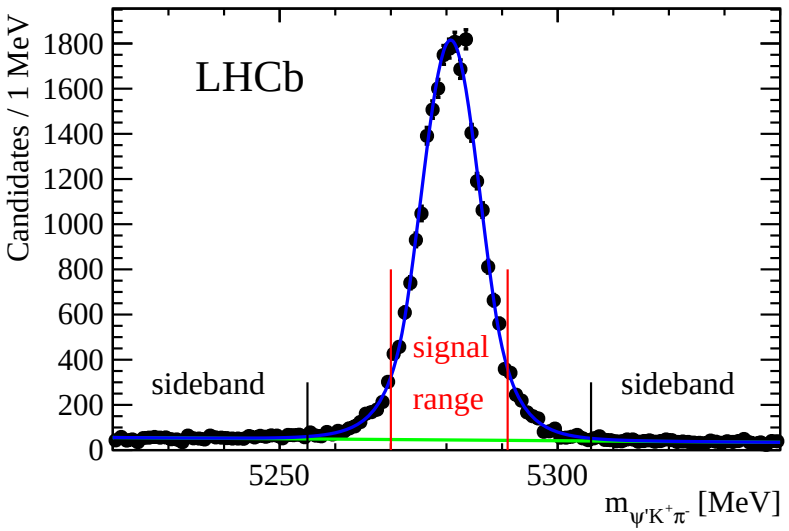

background subtracted Dalitz plot

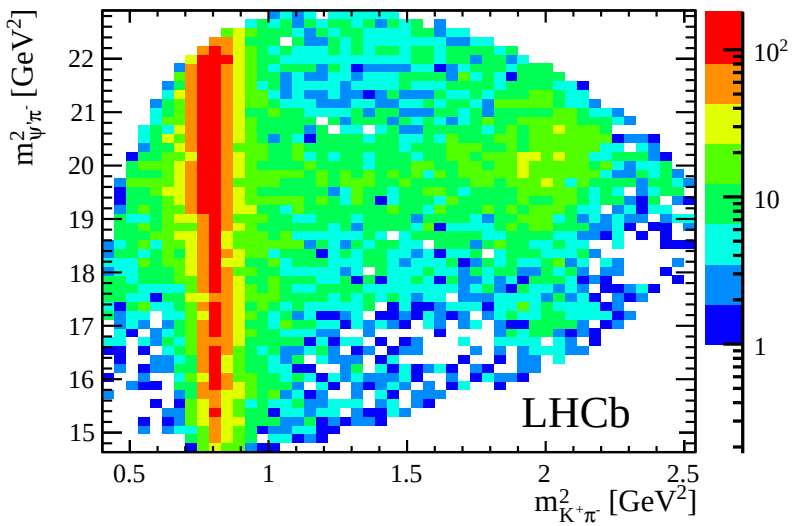

$Z(4430)^+$
Amplitude fit

- Fitted parameters:

$$M_{Z(4430)^+} = 4475 \pm 7^{+15}_{-25}\,\mathrm{MeV}/c^2, \Gamma_{Z(4430)^+} = 172 \pm 13^{+37}_{-34}\,\mathrm{MeV}/c^2$$

$$f_{Z(4430)^+} = (5.9 \pm 0.9^{+1.5}_{-3.3})\%$$

.

- Significance: $\Delta(-2lnL) > 13.9\sigma$

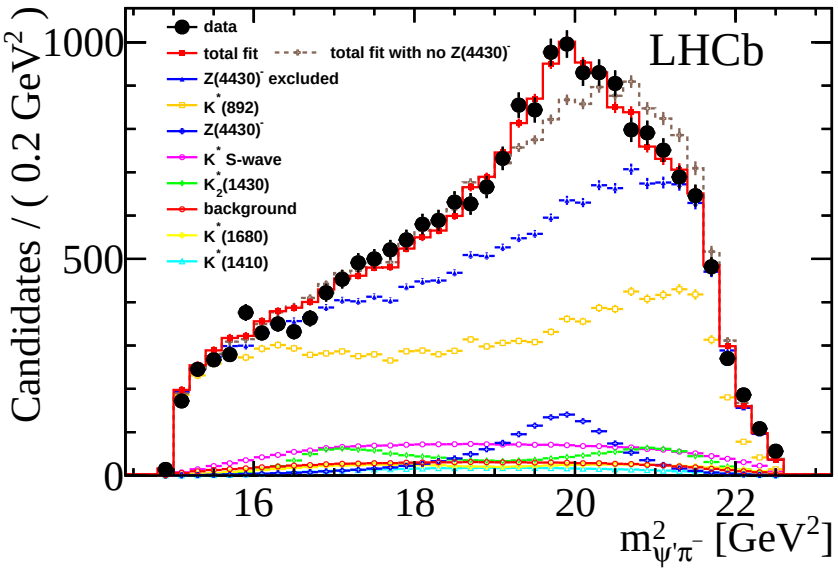

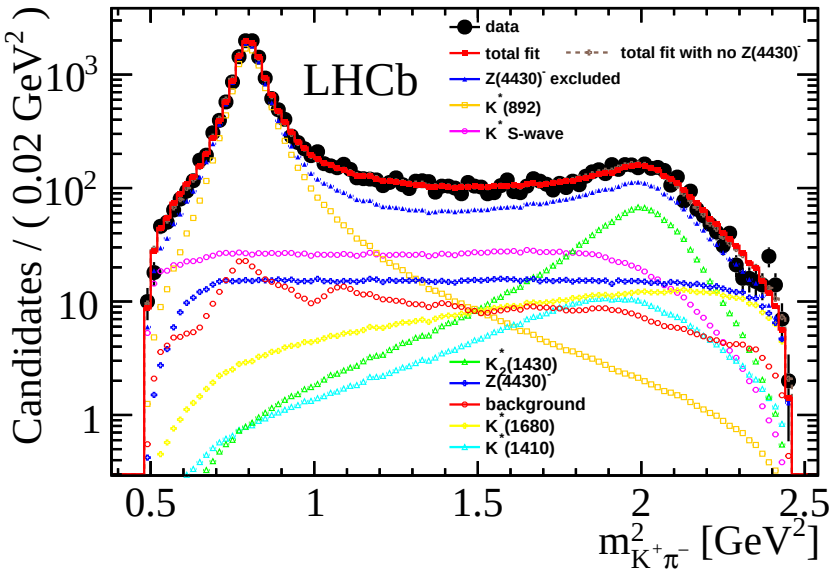

$Z(4430)^+$

Resonance character and spin determination

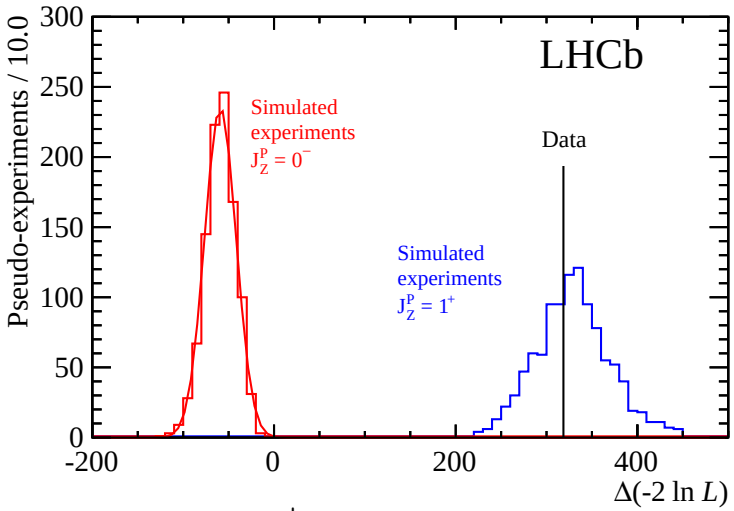

- $J^P = 1^+$ assignment favored.
- Other J^P assignments are ruled out with large significance: $> 9\sigma$

- $Z(4430)^+$ amplitude is described by 6 independent complex numbers instead of a Breit-Wigner
- Observe a fast change of phase crossing maximum of magnitude.
- Expected behaviour for a resonance.

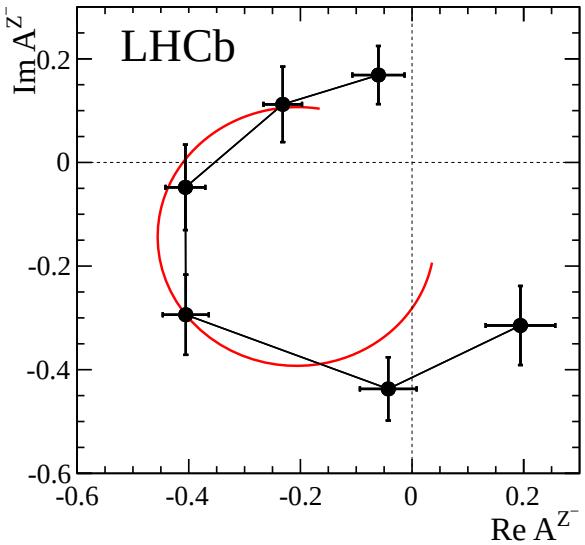

$Z(4430)^+$: model independent analysis

Phys. Rev. D 92, 112009 (2015)

The main goal is to check if the structures in the $\mathrm{m}_{\psi(2S)\pi}$ spectrum can be explained as reflections of the resonance activity in the $\mathrm{K}\pi$ system.

- No assumptions on the shape and coupling of the K^* resonances.
- Only its maximum J is restricted.

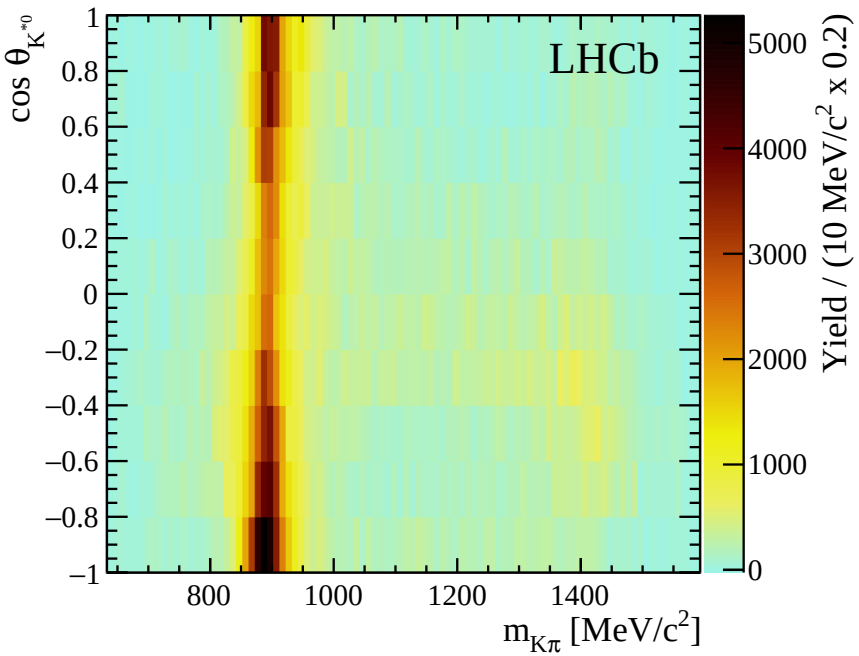

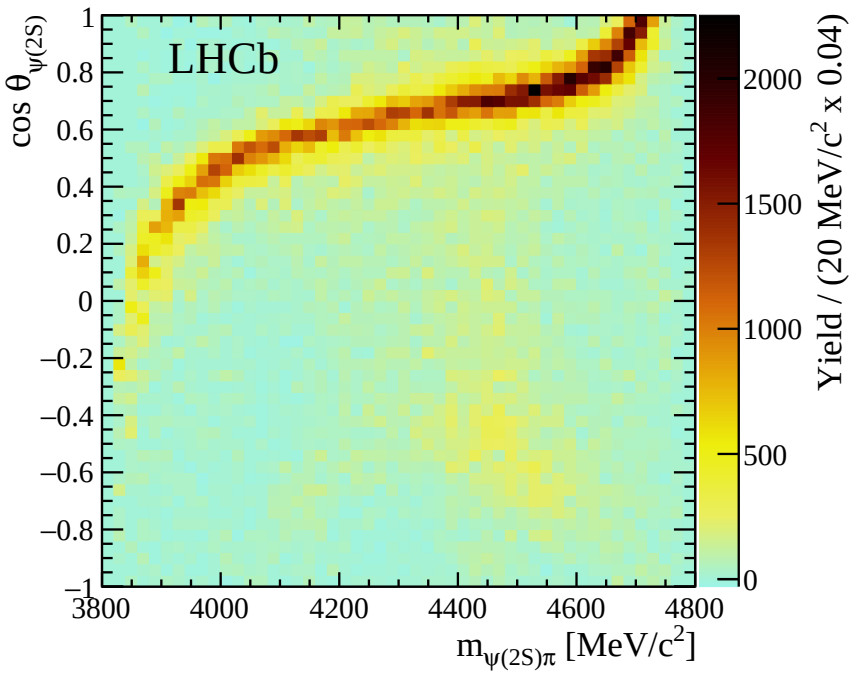

$Z(4430)^+$: model independent analysis

$K\pi$ system

- Very active $K\pi$ system.
- $m_{K\pi}$ taken directly from data, as it is.
- Angular structure of the $K\pi$ system acquired via Legendre polynomials.
- $\frac{dN}{d\cos\theta_{K^{*0}}} = \sum_{j=0}^{l_{max}} \langle P_j^U \rangle \mathrm{P}_j(\cos\theta_{K^{*0}})$
- $\langle P_j^U \rangle = \sum_{i=1}^{N_{reco}} \frac{W^i_{signal}}{\epsilon^i} \mathrm{P}_j(\cos\theta^i_{K^{*0}})$

Resonance	Mass (MeV/c^2)	Γ (MeV/c^2)	J^P
$K^*(800)^0$	682±29	547±24	0^+
$K^*(892)^0$	895.81±0.19	47.4±0.6	1^-
$K^*(1410)^0$	1414±15	232±21	1^-
$K_0^*(1430)^0$	1425±50	270±80	0^+
$K_2^*(1430)^0$	1432.4±1.3	109±5	2^+
$K^*(1680)^0$	1717±27	322±110	1^-
$K_3^*(1780)^0$	1776±7	159±21	3^-

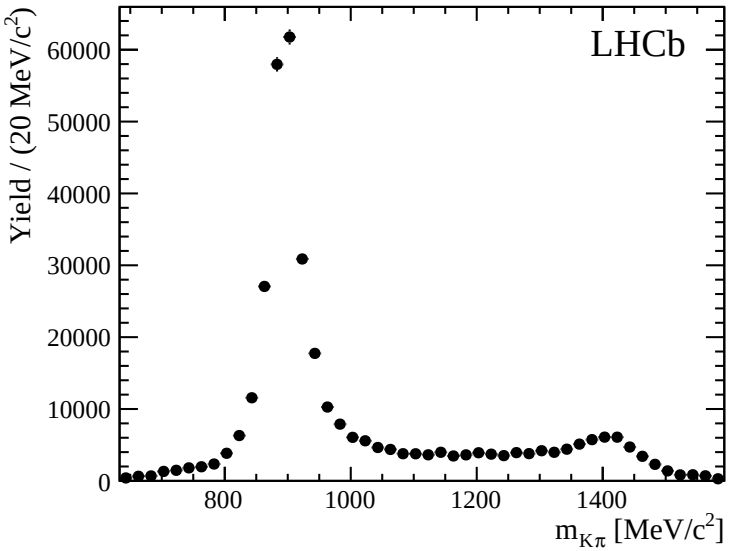

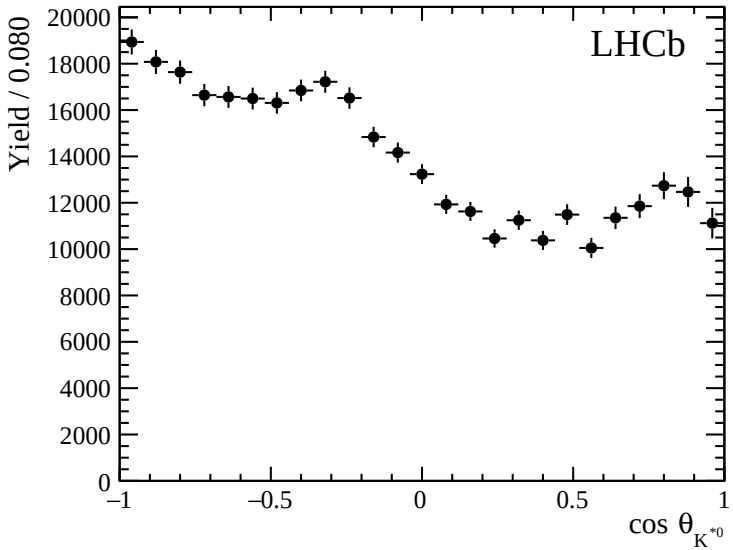

$Z(4430)^+$: model independent analysis

Legendre polynomial moments

The rich angular structure of the $K\pi$ system is shown by the very featured Legendre polynomial moments.

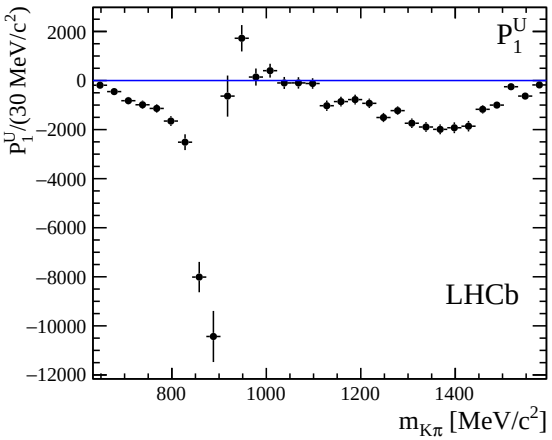

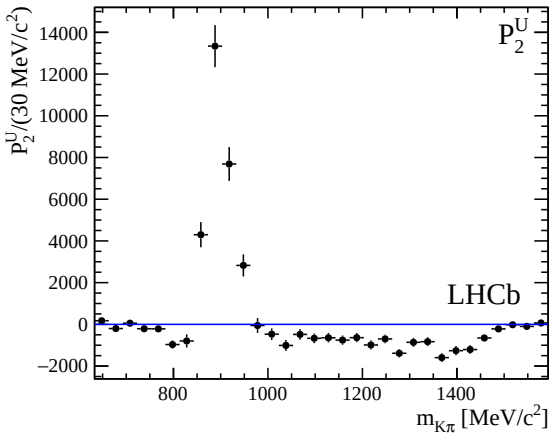

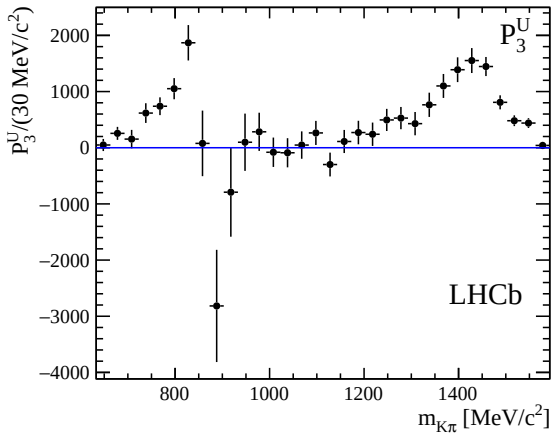

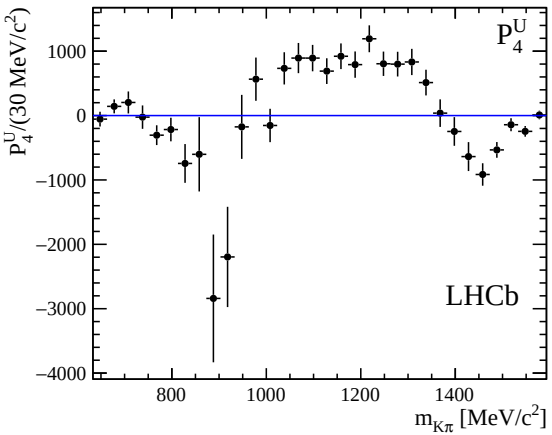

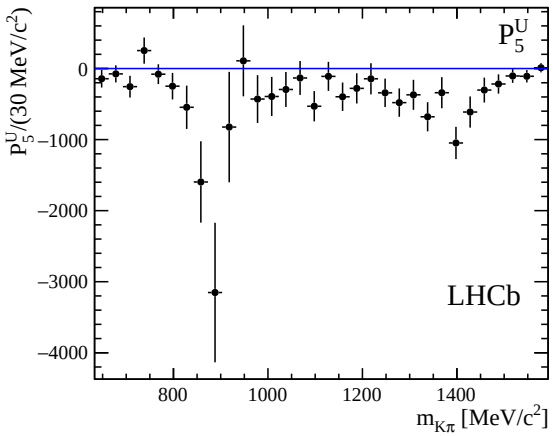

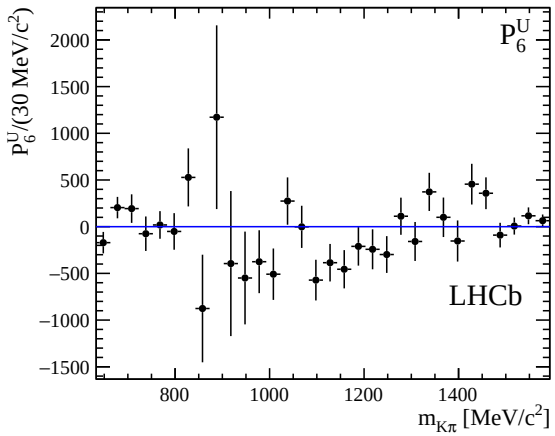

$Z(4430)^+$: model independent analysis

$m_{\psi(2S)\pi}$ spectrum

- The moments are normalized and used to predict, through a MC simulation, the expected $m_{\psi(2S)\pi}$ spectrum.
- The order of the Legendre polynomial expansion depends on the locally dominant $K\pi$ resonances

$$l_{\max}(m_{K\pi}) = \begin{cases} 2 & m_{K\pi} < 836\,\mathrm{MeV}/c^2 \\ 3 & 836\,\mathrm{MeV}/c^2 < m_{K\pi} < 1000\,\mathrm{MeV}/c^2 \\ 4 & m_{K\pi} > 1000\,\mathrm{MeV}/c^2. \end{cases}$$

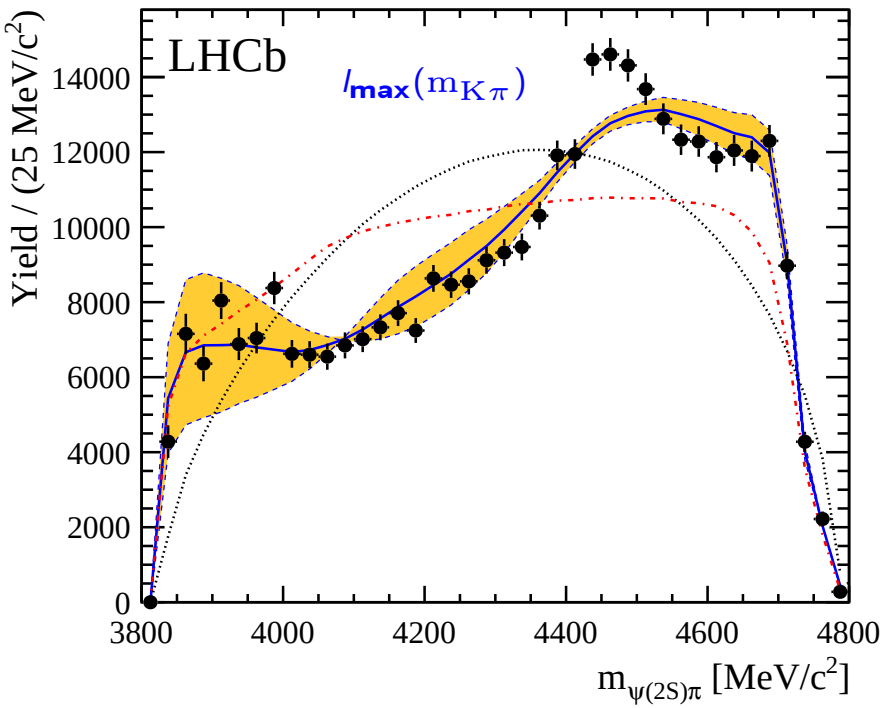

- **Data points(black dots)**
- **MC prediction (blue solid line)**
- Phase space MC (black dotted line)
- Phase space MC weighted to reproduce $m_{K\pi}$ (red line)

$Z(4430)^+$: model independent analysis

Slices of $m_{K\pi}$

Toy Monte Carlo prediction in slices of $m_{K\pi}$.

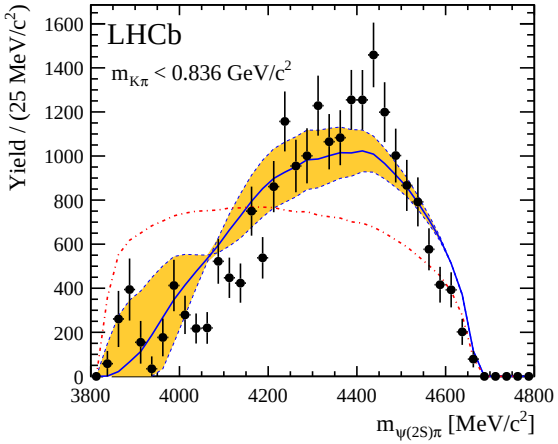

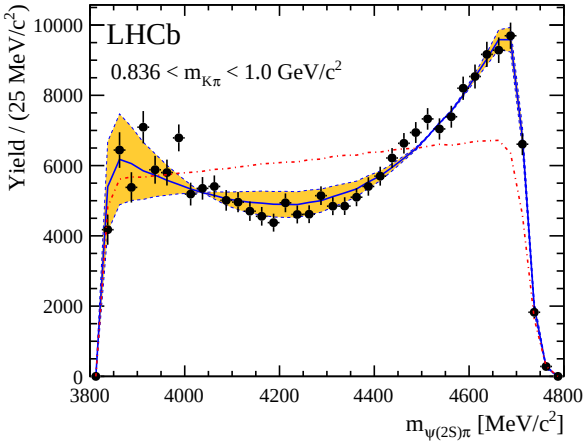

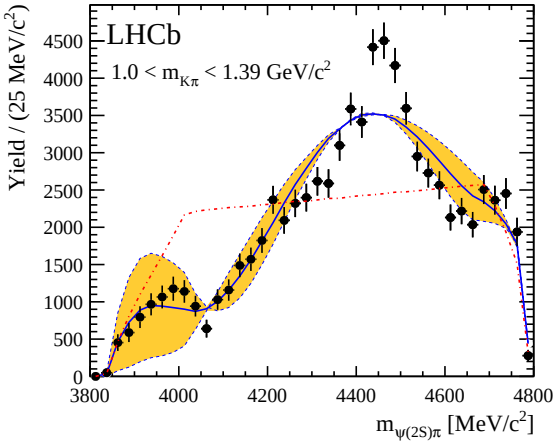

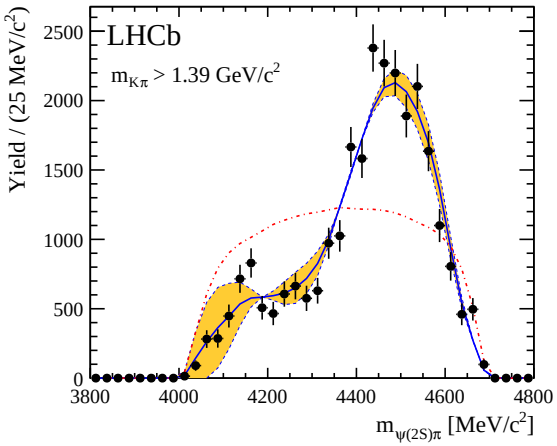

- **Data points(black dots)**
- **MC prediction (blue solid line)**
- Phase space MC weighted to reproduce $m_{K\pi}$ (red line)
- Clear disagreement between data and MC on the slice $1.0 < m_{K\pi} < 1.39\,\mathrm{GeV}/c^2$

$Z(4430)^+$: model independent analysis

Hypothesis test

- Performed using a series of pseudo-experiments produced according with J_{max} ($m_{K\pi}$).
- Hypothesis test based on likelihood ratio between J_{max} ($m_{K\pi}$) and J_{max} =30.
- Efficiency effects and background subtraction taken into account in the pseudo-experiment generation.

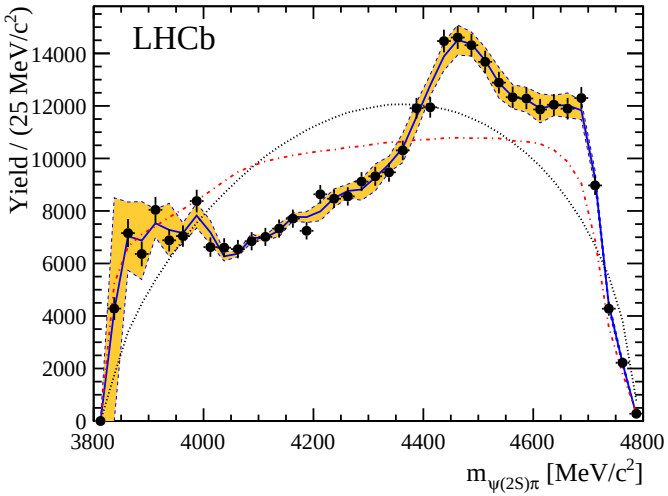

full $m_{K\pi}$ spectrum

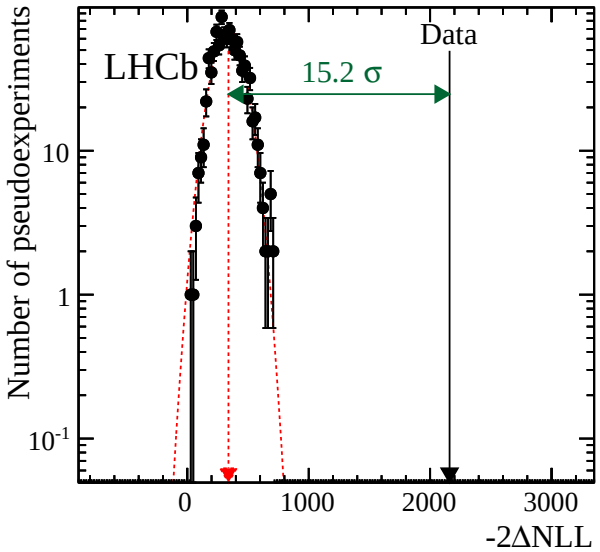

$1.0 < m_{K\pi} < 1.39\,\mathrm{GeV}/c^2$

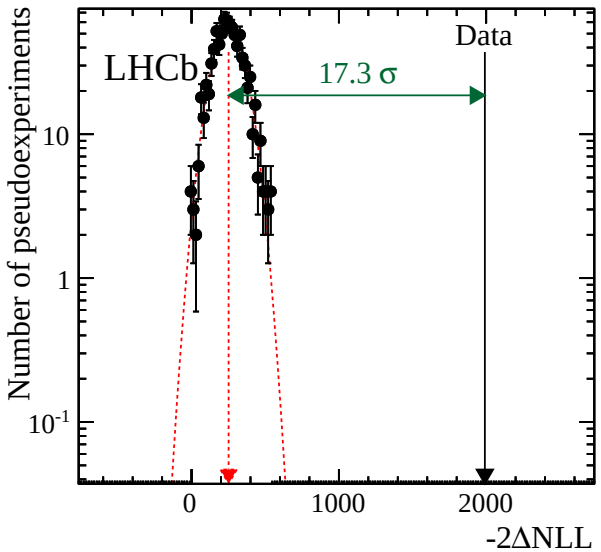

The hypotesis that the structure of the $m_{\psi(2S)\pi}$ spectrum can be described as a reflection of the activity of the resonances in the $K\pi$ system is ruled out with high significance.

$Z(4430)^+$: model independent analysis

Additional studies: $l_{max} \leq 4$

- Setting the maximum Legendre polynomial order to four, independent of $m_{K\pi}$
- This corresponds to suppose the $K\pi$ system has S,P and D waves contributing in all regions.
- Data can not be reproduced

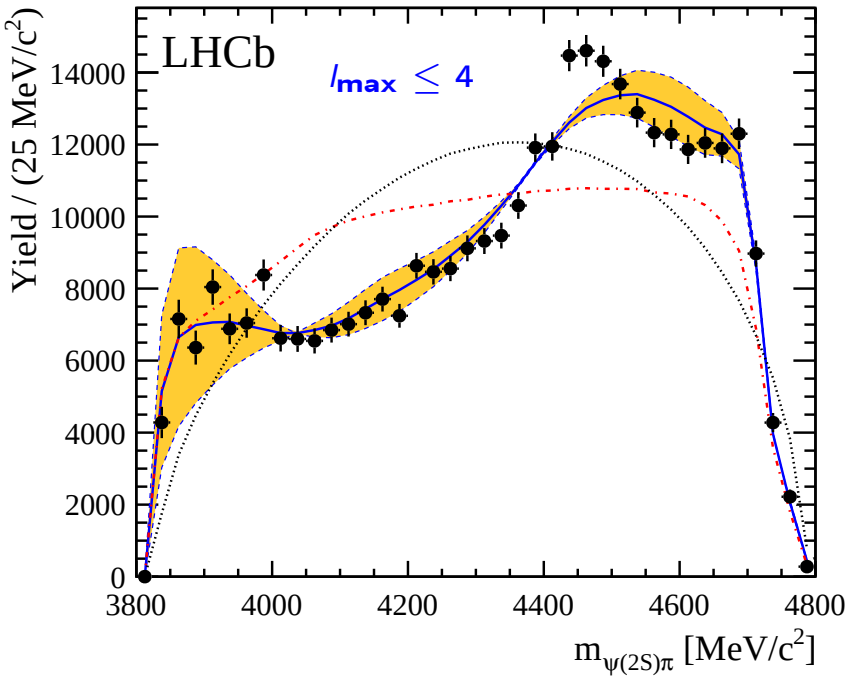

full $m_{K\pi}$ spectrum

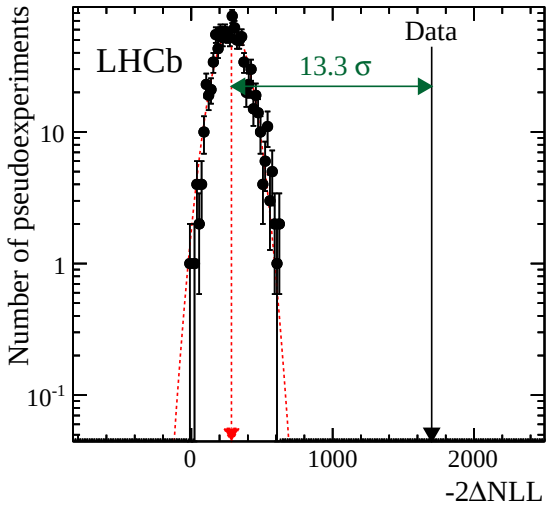

$1.0 < m_{K\pi} < 1.39\ \mathrm{GeV}/c^2$

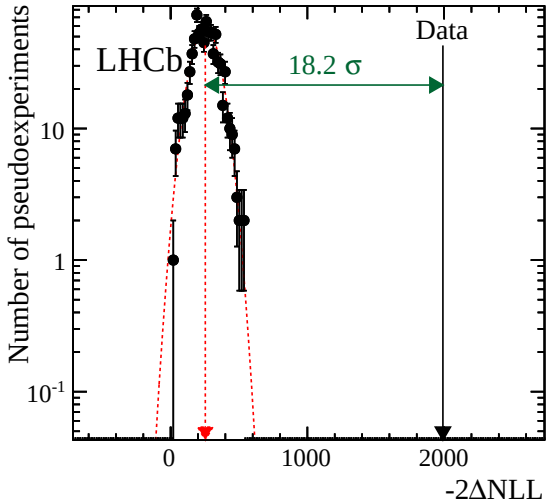

$Z(4430)^+$: model independent analysis

Additional studies: $l_{max} \leq 6$

- Setting the maximum Legendre polynomial order to six, independent of $\mathrm{m_{K\pi}}$
- This corresponds to suppose the $\mathrm{K\pi}$ system has S, P, D and F waves contributing in all regions.
- Data still can not be reproduced

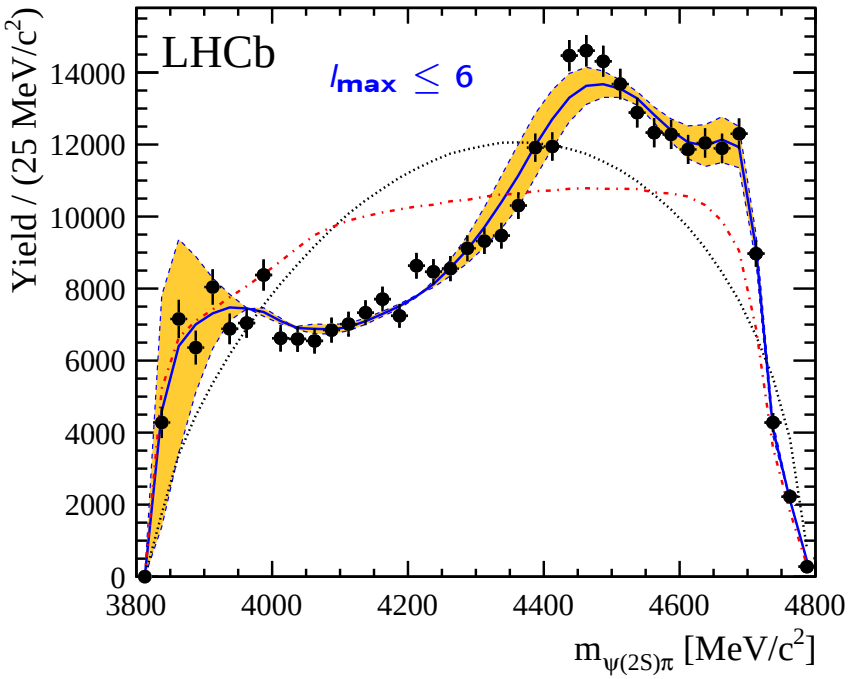

full $\mathrm{m_{K\pi}}$ spectrum

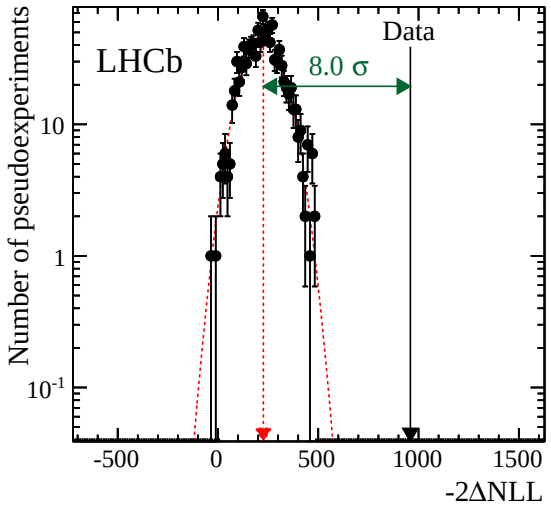

$1.0 < \mathrm{m_{K\pi}} < 1.39\ \mathrm{GeV}/c^2$

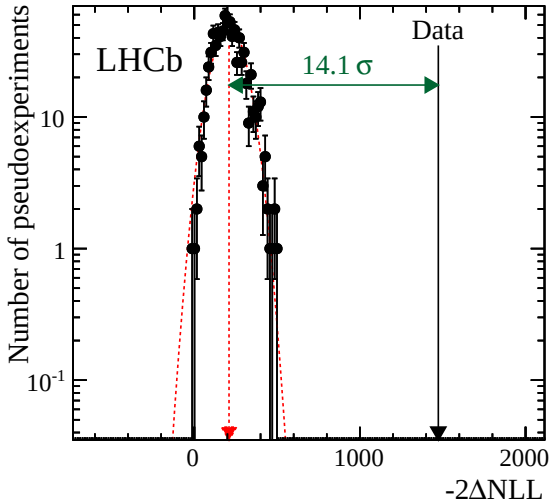

Quantum numbers of the X(3872) state and orbital angular momentum in its $\rho^0 J/\psi$ decays

Phys. Rev. D 92 (2015) 011102

- Previous quantum number determinations assumed that the lowest orbital angular momentum between the X(3872) decay products dominated the matrix element.
- Significant contributions from higher orbital angular amplitudes could invalidate the 1^{++} assignment. It is necessary to perform again the analysis allowing more general angular configurations.
- Using the 3.0 fb^{-1} dataset recorded by LHCb in 2011 and 2012
- 1011 ± 38 $B^+ \to K^+ X(3872)$ with $X(3872) \to J/\psi \pi^+ \pi^-$.
- 5D analysis: all angular correlations used to measure X(3872) J^{PC}

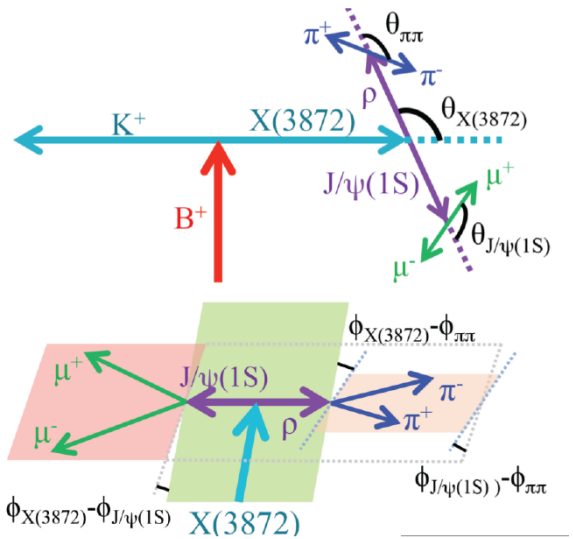

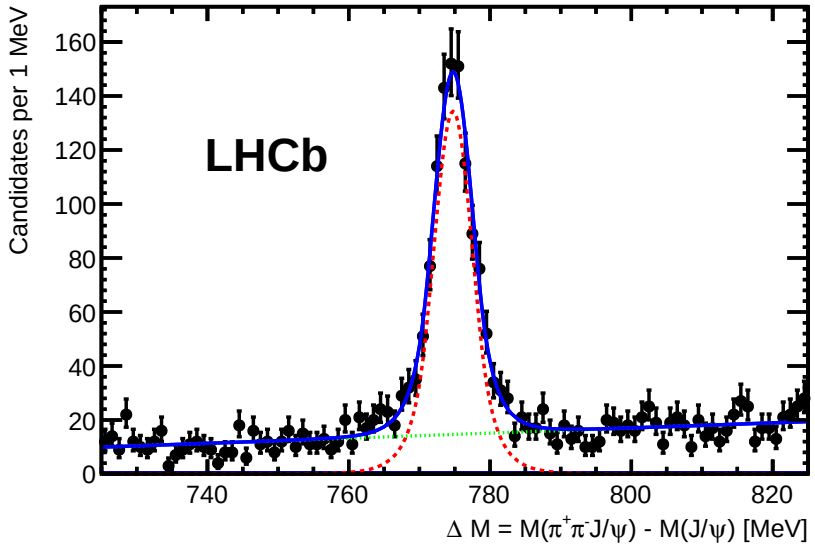

Quantum numbers of the X(3872) state and orbital angular momentum in its $\rho^0 J/\psi$ decays

Hypotesis test

- A large set of X(3872) J^{PC} configurations is considered.
- Likelihood-ratio test to discriminate between the assignments against the 1^{++};
- Results on data compared to simulated experiments.
- Data favour the 1^{++} over the alternative hypothesis with $> 16.0\sigma$;
- No significant D-wave fraction is found, with an upper limit of 0.4% at 95% C.L.

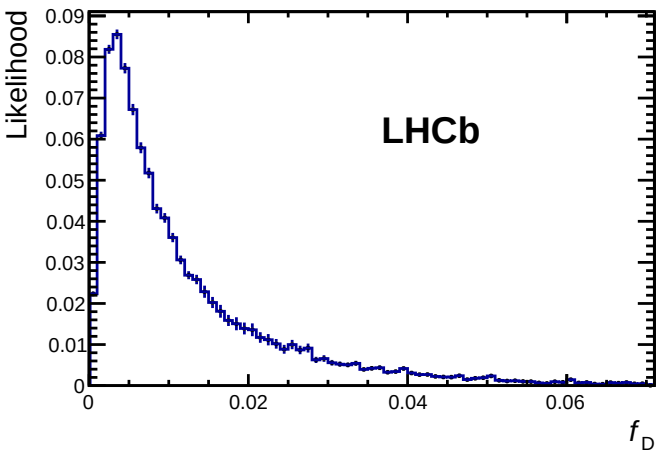

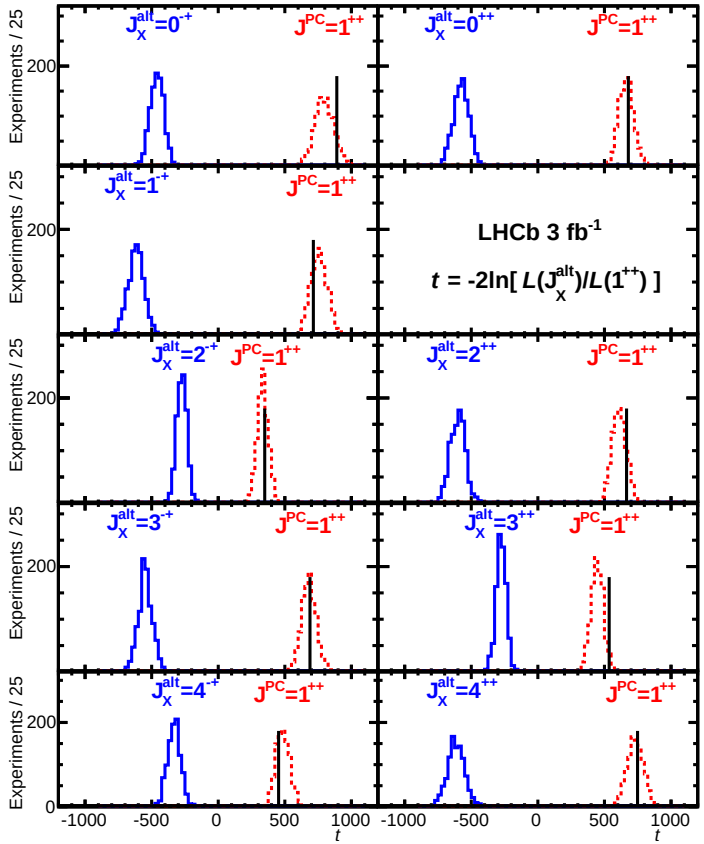

Quantum numbers of the X(3872) state and orbital angular momentum in its $\rho^0 J/\psi$ decays

Angular distributions

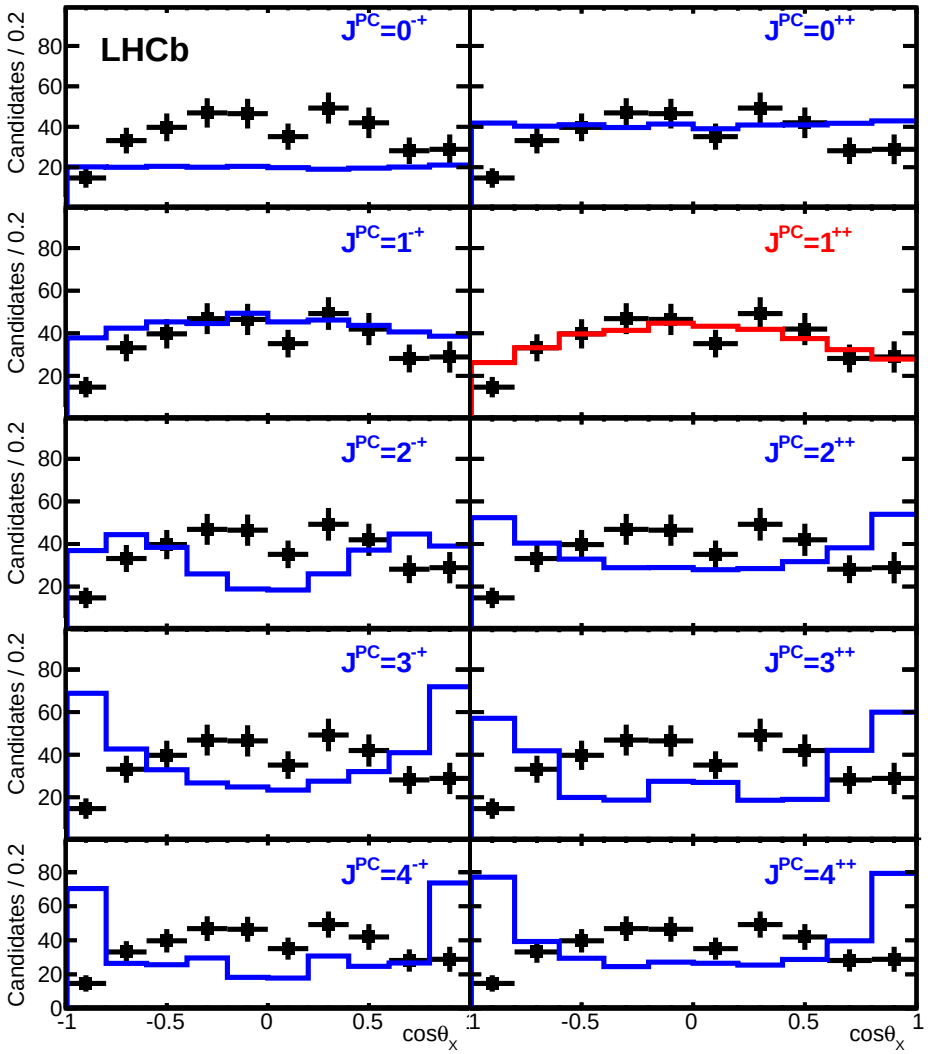

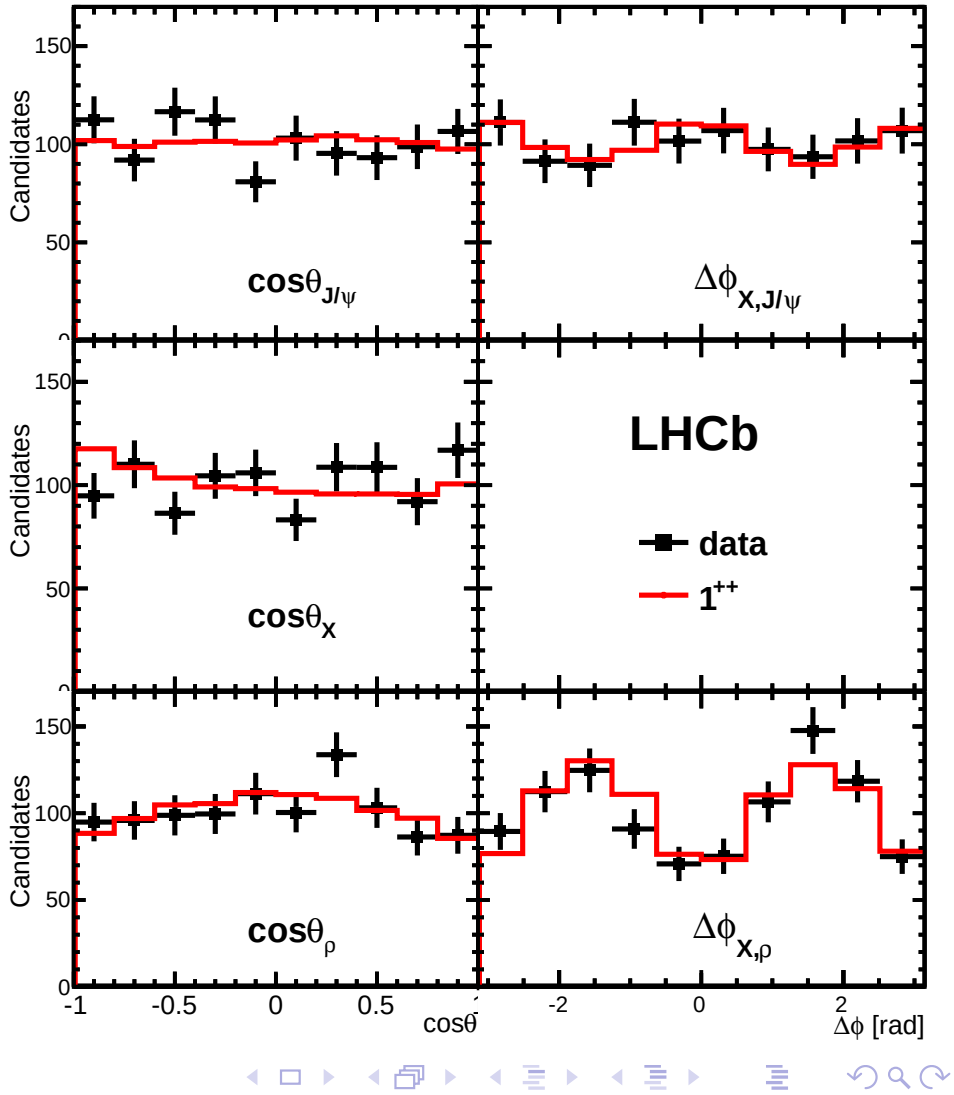

$B^0 \to J/\psi \pi^+\pi^-$

Phys. Rev. D 87, 052001

- The substructure of mesons belonging to the scalar nonet is controversial.
- Many possibilities: $q\bar{q}$, $q\bar{q}q\bar{q}$, mixtures etc.
- $q\bar{q}$ case:

$$\begin{aligned} |f_0(980)\rangle &= \cos\varphi_m |s\bar{s}\rangle + \sin\varphi_m |n\bar{n}\rangle \\ |f_0(500)\rangle &= -\sin\varphi_m |s\bar{s}\rangle + \cos\varphi_m |n\bar{n}\rangle, \\ \text{where } |n\bar{n}\rangle &\equiv \frac{1}{\sqrt{2}}\left(|u\bar{u}\rangle + |d\bar{d}\rangle\right). \end{aligned}$$

- $q\bar{q}q\bar{q}$ case:

$$\begin{aligned} |f_0(980)\rangle &= \frac{1}{\sqrt{2}}\left(|[su][\bar{s}\,\bar{u}]\rangle + |[sd][\bar{s}\bar{d}]\rangle\right) \\ |f_0(500)\rangle &= |[ud][\bar{u}\bar{d}]\rangle. \end{aligned}$$

- Observable of interest for both cases:

$$\tan^2\varphi_m \equiv r_\sigma^f = \frac{\mathcal{B}\left(\overline{B}^0 \to J/\psi\, f_0(980)\right)}{\mathcal{B}\left(\overline{B}^0 \to J/\psi\, f_0(500)\right)} \frac{\Phi(500)}{\Phi(980)}$$

- Prediction for tetraquark states: $r_\sigma^f = 1/2$ [PRL 111, 062001 (2013)]

$B^0 \to J/\psi \pi^+\pi^-$

Amplitude analysis

- Approach similar to the $Z(4430)^+$ analysis: 4D matrix element describing π^+ π^- resonances;
- No evidence of $J/\psi \pi^+$ resonances
- 19,000 B^0 signal candidates
- Background modelled from sidebands

Signal B^0 candidates in red.

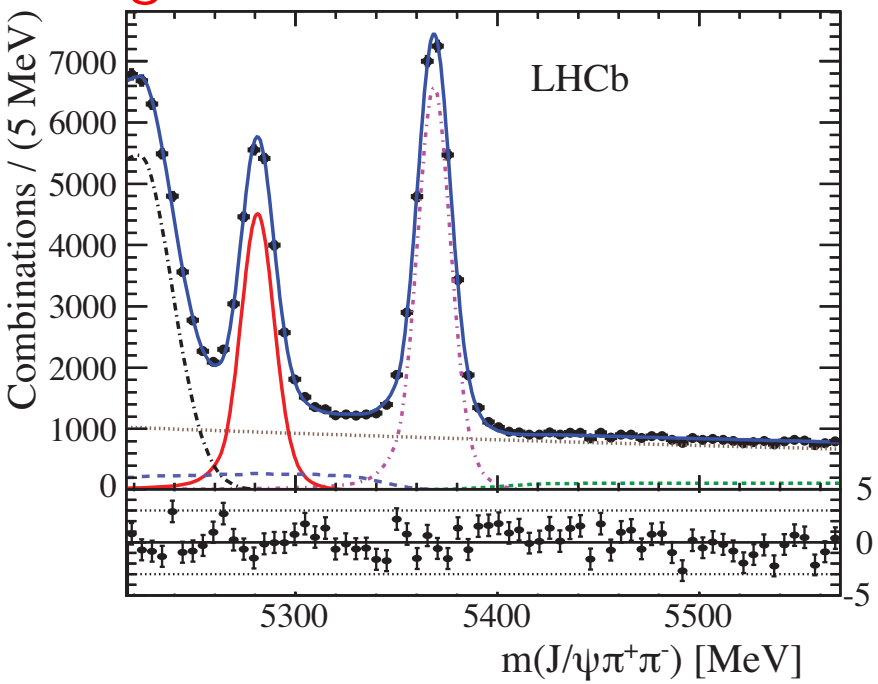

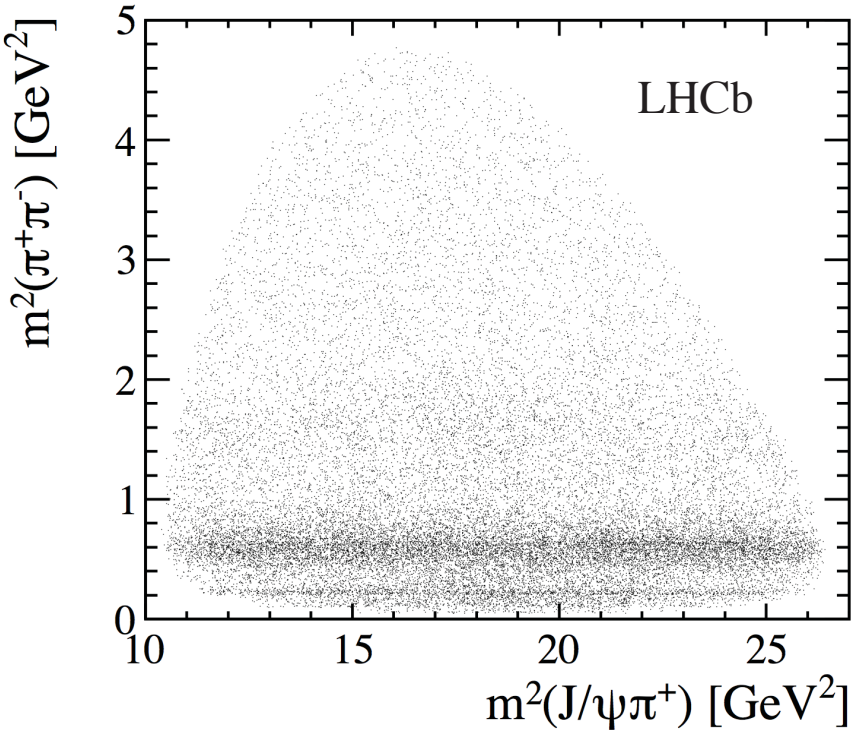

$B^0 \to J/\psi \pi^+\pi^-$

Results

R	$\mathcal{B}(\overline{B}^0 \to J/\psi R, R \to \pi^+\pi^-)$
$\rho(770)$	$(2.50 \pm 0.10^{+0.18}_{-0.15}) \times 10^{-5}$
$f_0(500)$	$(8.8 \pm 0.5^{+1.1}_{-1.5}) \times 10^{-6}$
$f_2(1270)$	$(3.0 \pm 0.3^{+0.2}_{-0.3}) \times 10^{-6}$
$\omega(782)$	$(2.7^{+0.8+0.7}_{-0.6-0.5}) \times 10^{-7}$
$\rho(1450)$	$(4.6 \pm 1.1 \pm 1.9) \times 10^{-6}$
$\rho(1700)$	$(2.0 \pm 0.5 \pm 1.2) \times 10^{-6}$

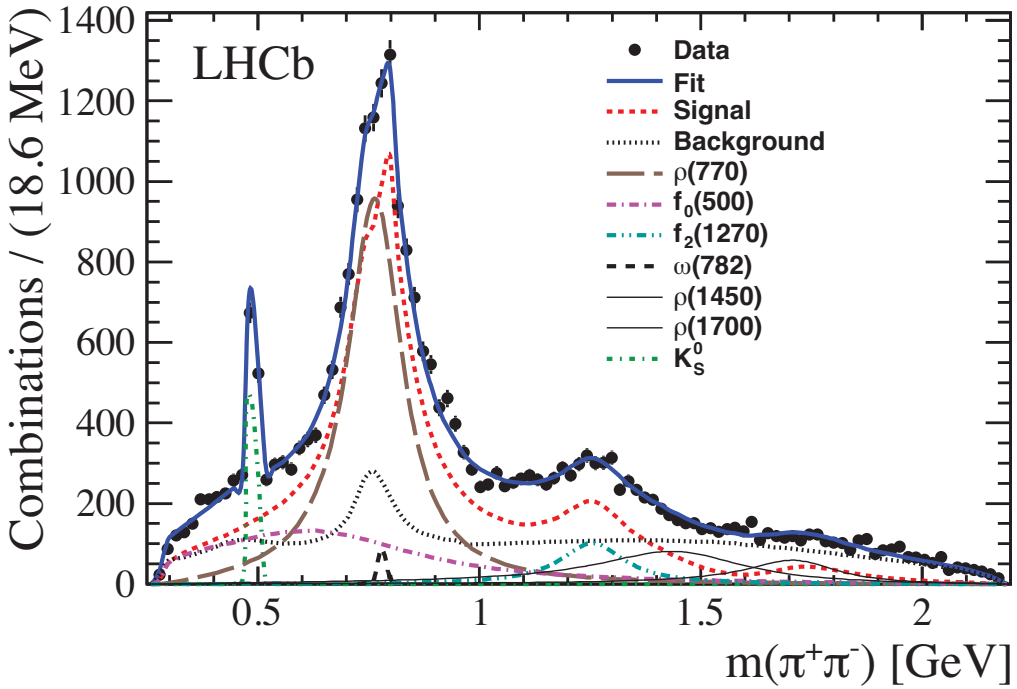

- Best fit model shows does not require $f_0(980)$ component.
- Upper limit on the $f_0(500) - f_0(980)$ mixing angle.
- Different from tetraquark prediction (1/2) by 8σ

$$\tan^2 \varphi_m \equiv r_\sigma^f = \left(1.1^{+1.2+6.0}_{-0.7-0.7}\right) \times 10^{-2} < 0.098 \quad \text{at } 90\% \text{ C.L}$$

Previous results:

- $\mathrm{X}(3872)$ **mass and production cross-section measurements [Eur. Phys. J. C. 72 (2012) 1972].** There is work in progress to update the mass measurement using the full dataset.
- $\mathrm{X}(3872)$ **quantum numbers determination [Phys. Rev. Lett. 110, 222001 (2013)].** In this analysis the decay of $\mathrm{X}(3872)$ was supposed to proceed only via $\rho\mathrm{J}/\psi$ S wave. Updated result discussed in the previous slides.
- **Search for** $\mathrm{X}(3872)$ **and** $\mathrm{X}(3915)$ **in** $\mathrm{B}^+ \to \mathrm{K}^+\mathrm{p}\overline{\mathrm{p}}$ **[Eur.Phys.J. C73 (2013) 2462].**
- **Evidence of** $\mathrm{X}(3872) \to \psi(2S)\gamma$ **[Nuclear Physics B 886 (2014) 665-680].** Update with 2016 statictics.
- **Results on** $\mathrm{X}(4140)$ **and** $\mathrm{X}(4274)$ **at LHCb [Phys. Rev. D 85,091103(R)(2012)].** Full amplitude analysis in progress using the full dataset.

There is intesive activity inside the LHCb searching for new multiquark candidates.

Many other results in b and c spectroscopy

Access: http://lhcbproject.web.cern.ch/lhcbproject/Publications/LHCbProjectPublic/Summary_all.html

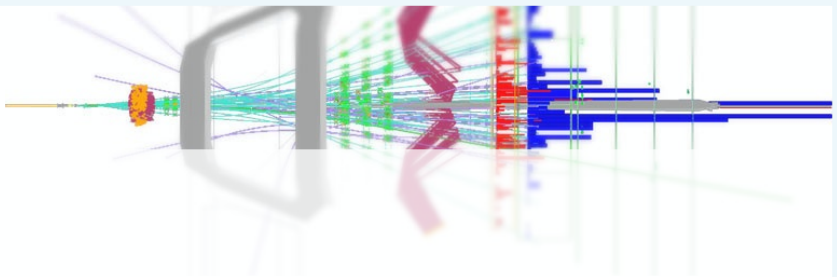

The LHCb Public results

LHCb publications

[to restricted-access page]

PUBLICATIONS PER WORKING GROUP

- FLAVOUR TAGGING
- b-HADRONS AND QUARKONIA
- B DECAYS TO CHARMONIUM
- DETECTOR PERFORMANCE
- CHARMLESS b-HADRON DECAYS
- QCD, ELECTROWEAK AND EXOTICA
- RARE DECAYS
- CHARM PHYSICS
- SEMILEPTONIC B DECAYS
- LUMINOSITY
- B DECAYS TO OPEN CHARM

List of papers (Total of 284 papers)

TITLE	DOCUMENT NUMBER	JOURNAL	SUBMITTED ON
Search for the rare decays $B^0 \to J/\psi\gamma$ and $B_s^0 \to J/\psi\gamma$	PAPER-2015-044	PRD	16 Oct 2015
Evidence for the strangeness-changing weak decay $\Xi_b^- \to \Lambda_b^0\pi^-$	PAPER-2015-047	PRL	13 Oct 2015
A model-independent confirmation of the $Z(4430)^-$ state	PAPER-2015-038	PRD	07 Oct 2015
Measurements of prompt charm production cross-sections in pp collisions at $\sqrt{s} = 13$TeV	PAPER-2015-041	JHEP	06 Oct 2015
Model-independent measurement of mixing parameters in $D^0 \to K_S\pi^+\pi^-$ decays	PAPER-2015-042	JHEP	06 Oct 2015
Measurement of the forward-backward asymmetry in $Z/\gamma^* \to \mu^+\mu^-$ decays and determination of the effective weak mixing angle	PAPER-2015-039	JHEP	25 Sep 2015
Studies of the resonance structure in $D^0 \to K_S^0K^\pm\pi^\mp$ decays	PAPER-2015-026	PRD	22 Sep 2015
Forward production of Υ mesons in pp collisions at $\sqrt{s} = 7$ and 8TeV	PAPER-2015-045	JHEP	08 Sep 2015
Measurement of forward J/ψ production cross-sections in pp collisions at $\sqrt{s} = 13$ TeV	PAPER-2015-037	JHEP	02 Sep 2015
First measurement of the differential branching fraction and CP asymmetry of the $B^\pm \to \pi^\pm\mu^+\mu^-$ decay	PAPER-2015-035	JHEP	01 Sep 2015
Measurement of CP violation parameters and polarisation fractions in $B_s^0 \to J/\psi\overline{K}^{*0}$ decays	PAPER-2015-034	JHEP	01 Sep 2015
Study of the production of Λ_b^0 and $\overline{B}^0$ hadrons in pp collisions and first measurement of the $\Lambda_b^0 \to J/\psi pK^-$ branching fraction	PAPER-2015-032	Chin Phys C	01 Sep 2015
Measurement of the time-integrated CP asymmetry in $D^0 \to K_S^0K_S^0$ decays	PAPER-2015-030	JHEP	25 Aug 2015
Search for hidden-sector bosons in $B^0 \to K^{*0}\mu^+\mu^-$ decays	PAPER-2015-036	PRL	17 Aug 2015
Measurement of the $B_s^0 \to \phi\phi$ branching fraction and search for the decay $B^0 \to \phi\phi$	PAPER-2015-028	JHEP	04 Aug 2015
B flavour tagging using charm decays at the LHCb experiment	PAPER-2015-027	JINST	28 Jul 2015
Measurement of the branching fraction ratio $\mathcal{B}(B_c^+ \to \psi(2S)\pi^+)/\mathcal{B}(B_c^+ \to J/\psi\pi^+)$	PAPER-2015-024	PRD	13 Jul 2015
Observation of $J/\psi p$ resonances consistent with pentaquark states in $\Lambda_b^0 \to J/\psi K^- p$ decays	PAPER-2015-029	Phys. Rev. Lett. 115 (2015) 072001	13 Jul 2015
Search for long-lived heavy charged particles using a ring imaging Cherenkov technique at LHCb	PAPER-2015-002	JHEP	30 Jun 2015
Angular analysis and differential branching fraction of the decay $B_s^0 \to \phi\mu^+\mu^-$	PAPER-2015-023	JHEP	29 Jun 2015

Summary

$P(4380)^+_c$ and $P(4450)^+_c$

- $P(4380)^+_c$ observed with 9.0σ in multidimensional amplitude fit. Quantum numbers $J^P = 3/2^-$
- $P(4450)^+_c$ observed with 12.0σ in multidimensional amplitude fit. Quantum numbers $J^P = 5/2^+$
- Resonance behavior observed for $P(4450)^+_c$. $P(4380)^+_c$ needs further studies.

$Z(4430)^+$

- Existence confirmed with $> 13.0\sigma$ in multidimensional amplitude fit.
- Existence confirmed with $> 8.0\sigma$ in model independent analysis.
- Quantum numbers determination $J^P = 1^+$
- Resonant behavior observed.

Summary

$\mathrm{X}(3872)$ quantum numbers

- Analysis of the $\mathrm{X}(3872)$ quantum numbers using full LHCb dataset
- Determination of the $\rho \mathrm{J}/\psi$ D wave fraction.

Light quark spectroscopy using $\mathrm{B}^0 \to \mathrm{J}/\psi \pi^+ \pi^-$

- No evidence for $f_0(980)$ resonance production
- $f_0(980)$ as a tetraquark state ruled out at $8\,\sigma$

Thanks!

Backup

$\Lambda_b^0 \to K^- p J/\psi$: Systematic uncertainties

Table 2: Summary of systematic uncertainties on P_c^+ masses, widths and fit fractions, and Λ^* fit fractions. A fit fraction is the ratio of the phase space integrals of the matrix element squared for a single resonance and for the total amplitude. The terms "low" and "high" correspond to the lower and higher mass P_c^+ states. The sFit/cFit difference is listed as a cross-check and not included as an uncertainty.

Source	M_0 (MeV)		Γ_0 (MeV)		Fit fractions (%)			
	low	high	low	high	low	high	$\Lambda(1405)$	$\Lambda(1520)$
Extended vs. reduced	21	0.2	54	10	3.14	0.32	1.37	0.15
Λ^* masses & widths	7	0.7	20	4	0.58	0.37	2.49	2.45
Proton ID	2	0.3	1	2	0.27	0.14	0.20	0.05
$10 < p_p < 100$ GeV	0	1.2	1	1	0.09	0.03	0.31	0.01
Nonresonant	3	0.3	34	2	2.35	0.13	3.28	0.39
Separate sidebands	0	0	5	0	0.24	0.14	0.02	0.03
J^P $(3/2^+, 5/2^-)$ or $(5/2^+, 3/2^-)$	10	1.2	34	10	0.76	0.44		
$d = 1.5 - 4.5$ GeV^{-1}	9	0.6	19	3	0.29	0.42	0.36	1.91
$L^{P_c}_{\Lambda_b^0}$ $\Lambda_b^0 \to P_c^+$ (low/high)K^-	6	0.7	4	8	0.37	0.16		
L_{P_c} P_c^+ (low/high) $\to J/\psi p$	4	0.4	31	7	0.63	0.37		
$L^{\Lambda_n^*}_{\Lambda_b^0}$ $\Lambda_b^0 \to J/\psi \Lambda^*$	11	0.3	20	2	0.81	0.53	3.34	2.31
Efficiencies	1	0.4	4	0	0.13	0.02	0.26	0.23
Change $\Lambda(1405)$ coupling	0	0	0	0	0	0	1.90	0
Overall	29	2.5	86	19	4.21	1.05	5.82	3.89
sFit/cFit cross check	5	1.0	11	3	0.46	0.01	0.45	0.13

$\Lambda_b^0 \to K^- p J/\psi$: Slices $m_{pJ/\psi}$

Figure 8: $m_{J/\psi p}$ in various intervals of m_{Kp} for the fit with two P_c^+ states: (a) $m_{Kp} < 1.55$ GeV, (b) $1.55 < m_{Kp} < 1.70$ GeV, (c) $1.70 < m_{Kp} < 2.00$ GeV, and (d) $m_{Kp} > 2.00$ GeV. The data are shown as (black) squares with error bars, while the (red) circles show the results of the fit. The blue and purple histograms show the two P_c^+ states. See Fig. 7 for the legend.

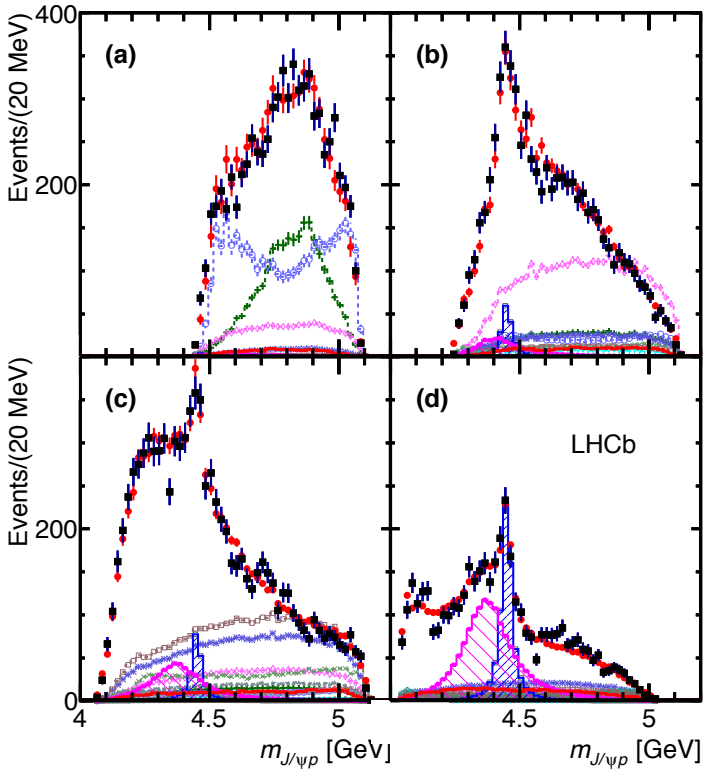

$\Lambda_b^0 \to K^- p J/\psi$: Slices $m_{KJ/\psi}$

Figure 11: Projections onto $m_{J/\psi K}$ in various intervals of m_{Kp} for the reduced model fit (cFit) with two P_c^+ states of J^P equal to $3/2^-$ and $5/2^+$: (a) $m_{Kp} < 1.55$ GeV, (b) $1.55 < m_{Kp} < 1.70$ GeV, (c) $1.70 < m_{Kp} < 2.00$ GeV, (d) $m_{Kp} > 2.00$ GeV, and (e) all m_{Kp}. The data are shown as (black) squares with error bars, while the (red) circles show the results of the fit. The individual resonances are given in the legend.

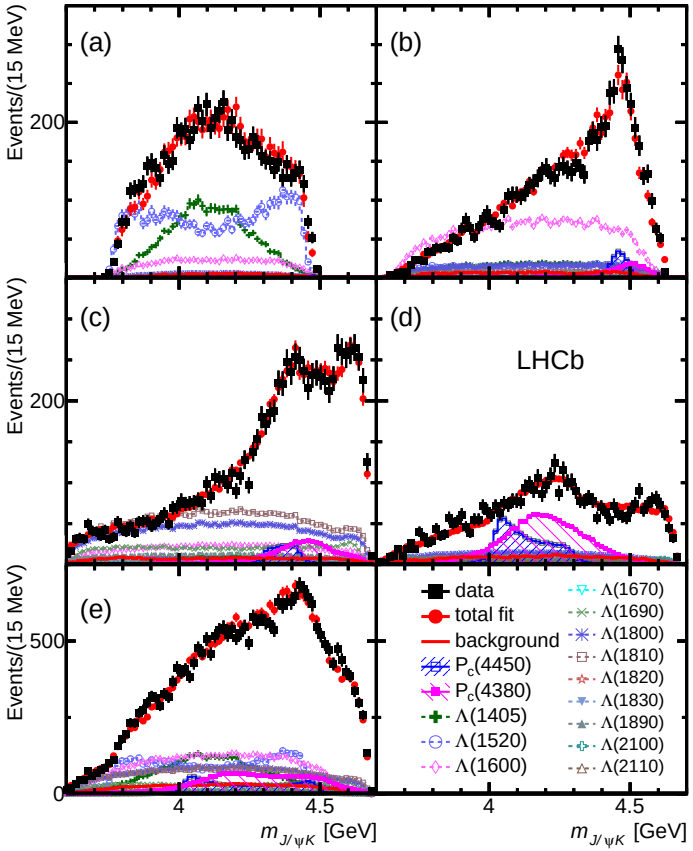

Backup: Older results

X(3872)

The X(3872) exotic-meson was discovered in 2003 by the Belle collaboration in $\mathrm{B} \to \mathrm{K X(3872)}$ with $\mathrm{X(3872)} \to \mathrm{J}/\psi\pi^+\pi^-$.

- Its existence was immediately confirmed by BaBar,CDF, DØ collaborations.
- Quantum numbers previously constrained to 1^{++} or 2^{-+}. It were just measured by LHCb as 1^{++}.
- Clear signature on the $\mathrm{X(3872)} \to \mathrm{J}/\psi\pi^+\pi^-$ mode. $\pi^+\pi^-$ mass spectrum well studied.
- Mass known to 0.2 MeV/c^2 and width $< 1.2\ \mathrm{MeV}/c^2$.

X(3872) signal at CDF

PRL 103,152001 (2009)

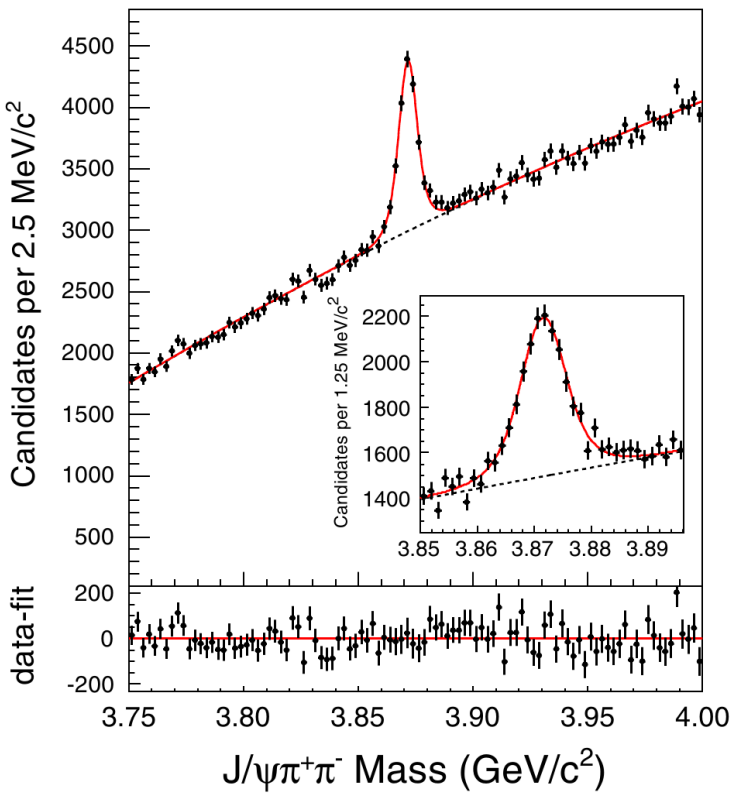

The nature of the X(3872) remains uncertain:

- Conventional charmonium $\chi_{c1}(2^3\mathrm{P}_1)$.(very unlikely)
- Mesonic molecular state: $D^{*0}\bar{D}^0$ bound state.
- Tetraquark (diquark-anti-diquark).

$\mathrm{X}(3872)$ production studies at LHCb

At LHCb, the $\mathrm{X}(3872)$ can be studied using:

- Prompt candidates: higher statistics but large combinatorial background.
- Candidates from B decays: lower statistics but more clear samples
- Both kinds of candidates (inclusive selection)

$\mathrm{X}(3872)$ production studies at LHCb:

- Measure $\sigma(\mathrm{pp} \to \mathrm{X}(3872) + \cdots) \times \mathcal{B}(\mathrm{X}(3872) \to \mathrm{J}/\psi\,\pi^+\pi^-)$
- $\mathrm{X}(3872)$ taken as a 1^{++} state
- Inclusive selection of $\mathrm{X}(3872) \to \mathrm{J}/\psi\,\pi^+\pi^-$
- Fiducial range: $5 < p_{\mathrm{T}} < 20$ GeV and $2.5 < \mathrm{y} < 4.5$
- Efficiency estimated from Monte Carlo

X(3872) production studies at LHCb

[Eur. Phys. J. C. 72 (2012) 1972]

Analysis performed on data sample with integrated luminosity of 34.7 pb^{-1} collected by the LHCb experiment in pp collisions at $\sqrt{s} = 7\ \text{TeV}$ in 2010.

$$\sigma(\text{pp} \to \text{X}(3872) + \cdots) \times \mathcal{B}(\text{X}(3872) \to \text{J}/\psi\,\pi^+\pi^-) = 5.4 \pm 1.3(\text{stat}) \pm 0.8(\text{syst})\,\text{nb}$$

$$\text{M}(X(3872)) = 3871.95 \pm 0.48(\text{stat}) \pm 0.12(\text{syst})\,\text{MeV}/c^2$$

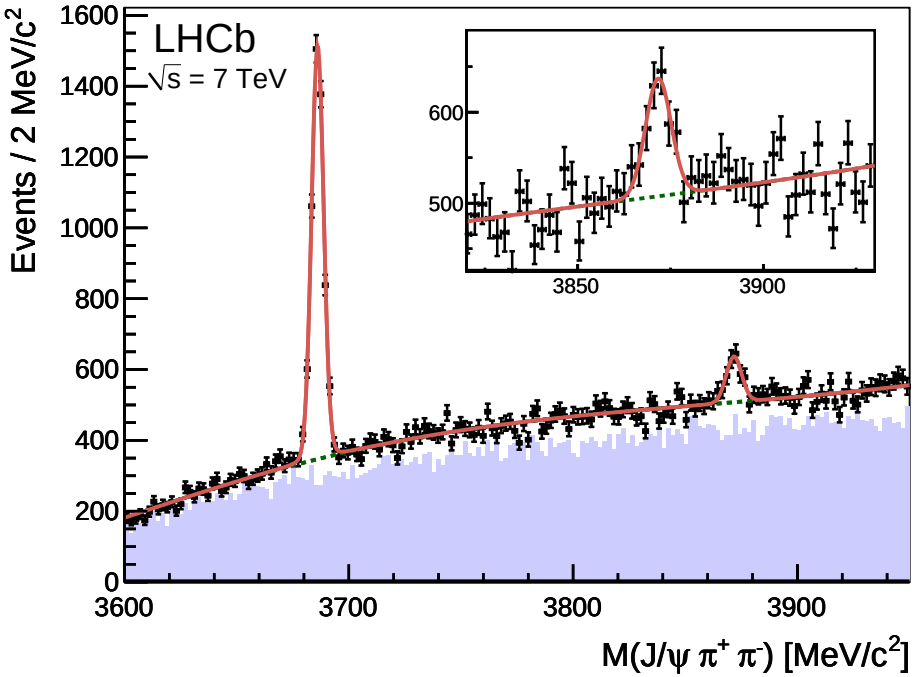

- 585 ± 74 $\text{X}(3872)$ signal candidates
- Momentum scale calibration using $\text{J}/\psi \to \mu^+\mu^-$.
- $\text{X}(3872)$ peak fitted with fixed width.
- Background studied from wrong-sign pions combinations and modeled by exponential function.
- Uncertainty dominated by statistics. It will improve with 2011 dataset

Status of X(3872) mass

- World average and $D^0\bar{D}^0*$-threshold are indistinguishable.
- Mass is a critical parameter for the $D^0\bar{D}^0*$-bound state hypotesis.
- Very low binding energy: $E_{bind} = 0.16 \pm 0.26\ \mathrm{MeV}/c^2$

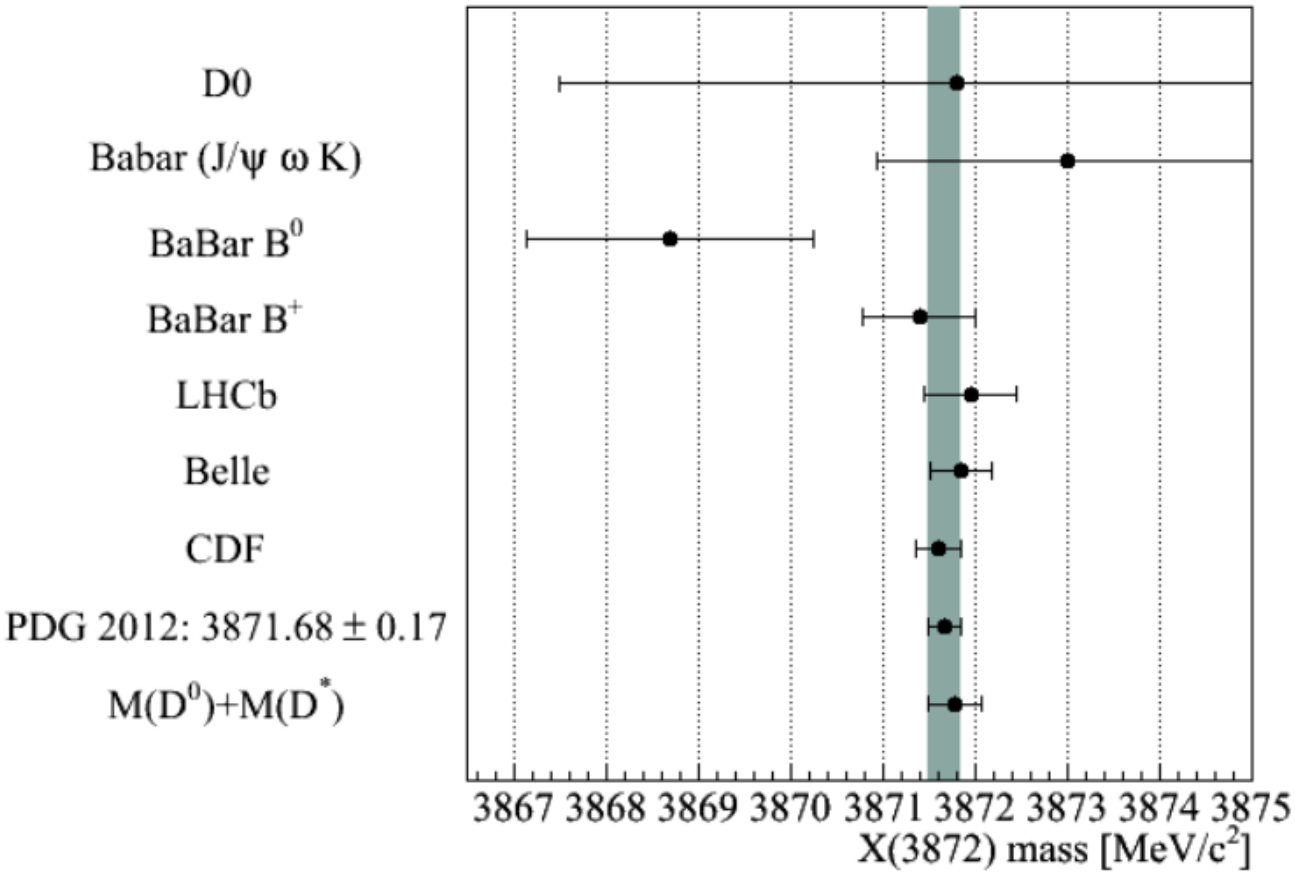

Precision D^0 mass measurement at LHCb

JHEP 1306 (2013) 065

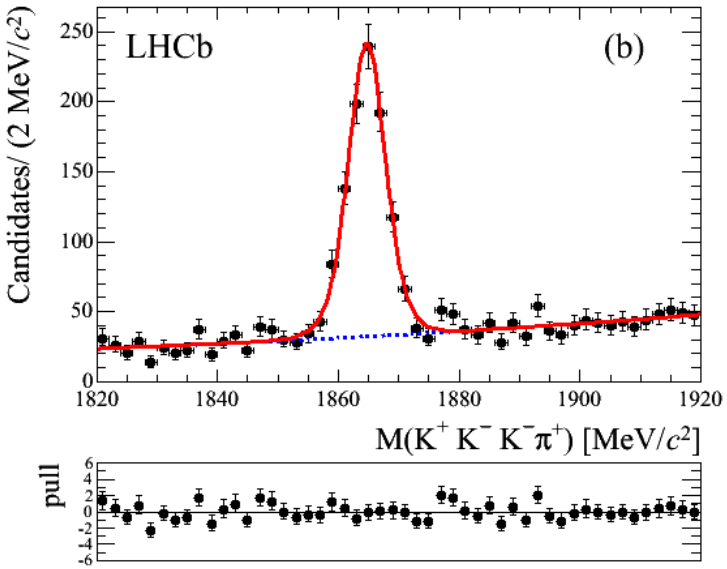

- D^0 mass measurement using D produced in semileptonic B decays
- Using $\mathrm{D}^0 \to \mathrm{K}^+\mathrm{K}^-\mathrm{K}^+\pi^-$
- 846 ± 36 events, low Q, low systematics

$$\mathrm{M}(\mathrm{D}^0) = 1864.75 \pm 0.15(\mathrm{stat}) \pm 0.11(\mathrm{syst})\ \mathrm{MeV}/c^2$$

- This result reinforces that if $\mathrm{X}(3872)$ is a $D^0\bar{D}^{0*}$ bound-state, it is loosely bound.
- Consistent with arxiv:1212.4191: $M(\mathrm{D}^0) = 1864.851 \pm 0.020(\mathrm{stat})$

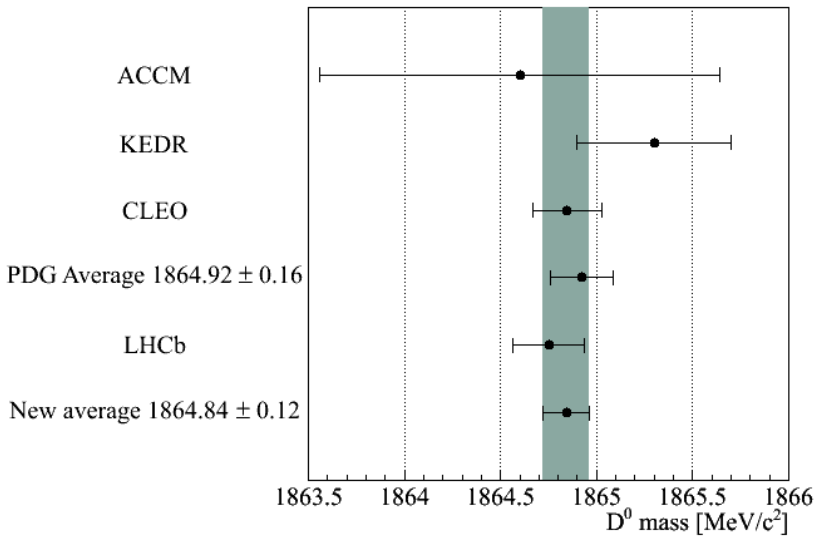

X(3872) quantum numbers determination

Phys. Rev. Lett. 110, 222001 (2013)

- Using the 1.0 fb^{-1} dataset recorded by LHCb in 2011
- 313 ± 26 $B^+ \to K^+X(3872)$ with $X(3872) \to J/\psi\pi^+\pi^-$.
- 5642 ± 76 $B^+ \to K^+\psi(2S)$ with $\psi(2S) \to J/\psi\pi^+\pi^-$.
- 5D analysis: all angular correlations used to measure X(3872) J^{PC}

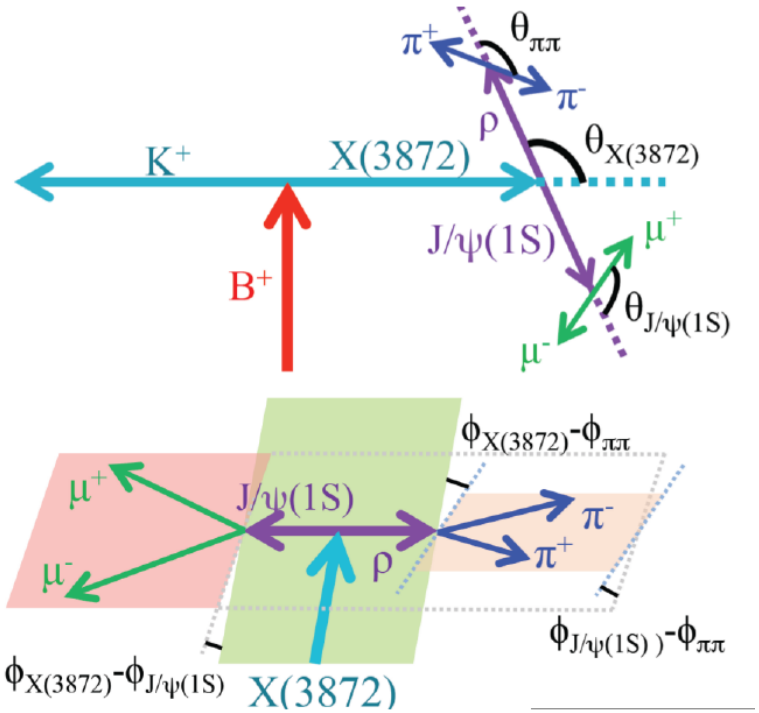

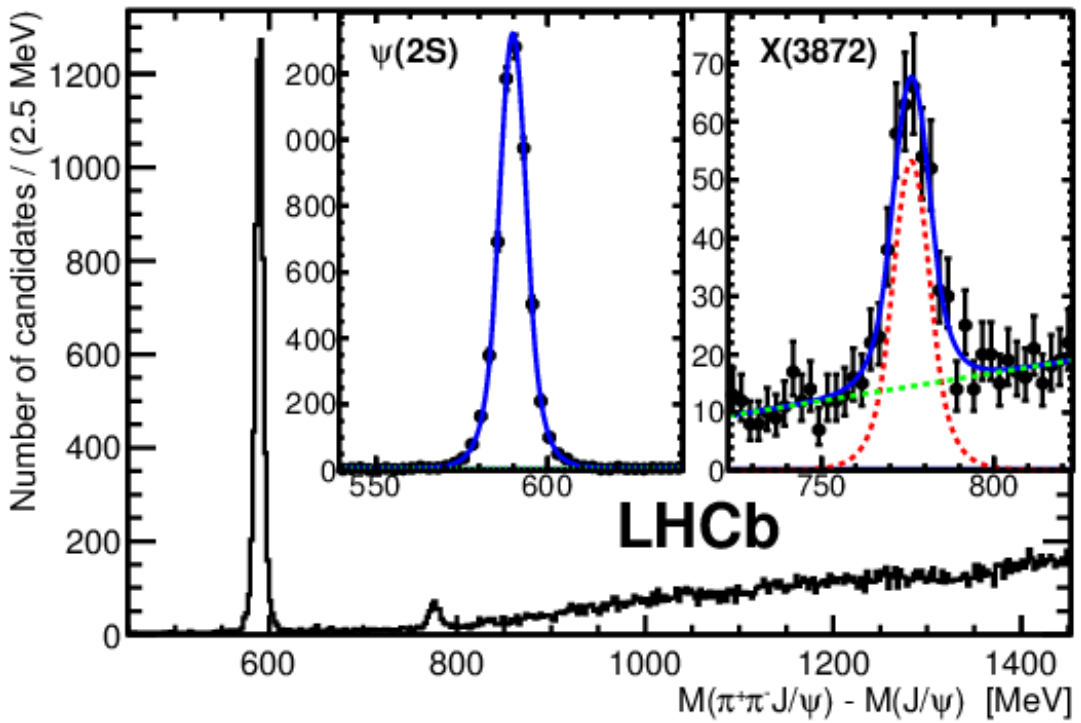

X(3872) quantum numbers determination

Phys. Rev. Lett. 110, 222001 (2013)

- Two X(3872) J^{PC} configurations are considered: 1^{++} and 2^{-+};
- Likelihood-ratio test, to discriminate between the assignments;
- Compare the results to simulated experiments;
- Data favour the 1^{++} over the 2^{-+} hypothesis at 8.4σ;

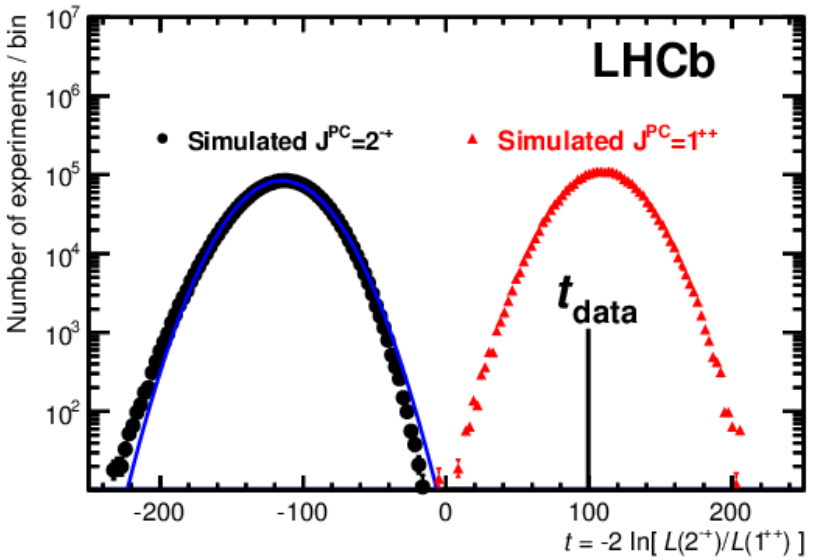

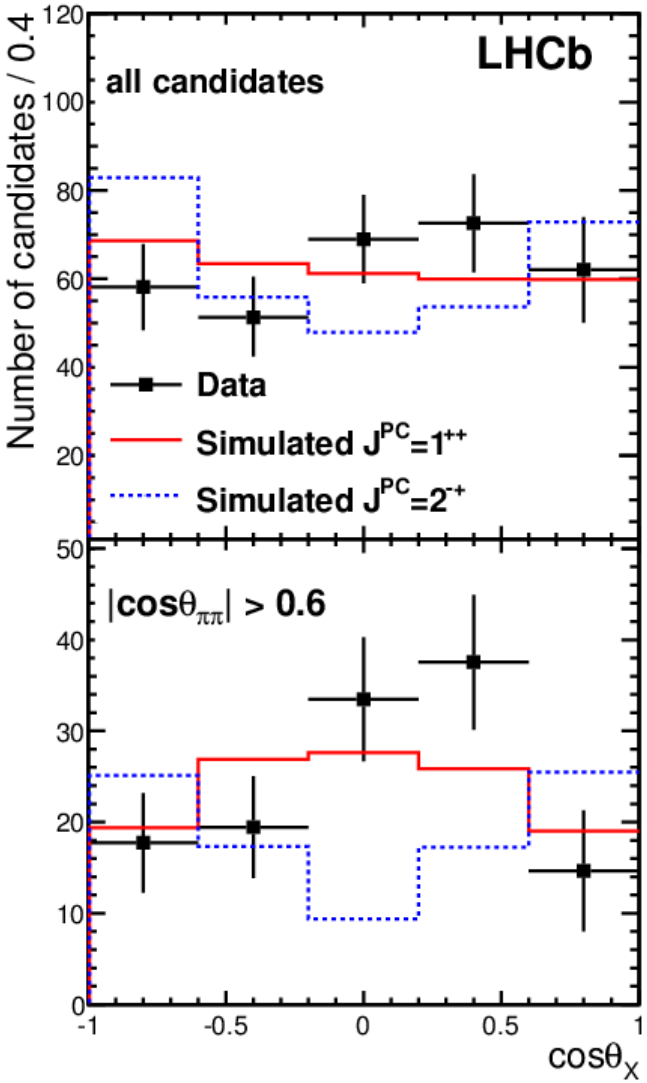

This result favours the interpretations of X(3872) as an exotic state.

Search for $\mathrm{X}(3872)$ and $\mathrm{X}(3915)$ in $\mathrm{B}^+ \to \mathrm{K}^+\mathrm{p}\overline{\mathrm{p}}$

Eur.Phys.J. C73 (2013) 2462

- Search for $\mathrm{B} \to \mathrm{KX}(3872)$ with $\mathrm{X}(3872) \to \mathrm{p}\overline{\mathrm{p}}$;
- 6951 ± 176 candidates of $\mathrm{B}^+ \to \mathrm{K}^+\mathrm{p}\overline{\mathrm{p}}$
- $-9 \pm 8(\mathrm{stat}) \pm 2(\mathrm{syst})$ candidates of $\mathrm{X}(3872) \to \mathrm{p}\overline{\mathrm{p}}$
- $13 \pm 17(\mathrm{stat}) \pm 5(\mathrm{syst})$ candidates of $\mathrm{X}(3915) \to \mathrm{p}\overline{\mathrm{p}}$
- $\frac{\mathcal{B}(\mathrm{B}^+ \to \mathrm{K}^+\mathrm{X}(3872)) \times \mathcal{B}(\mathrm{X}(3872) \to \mathrm{p}\overline{\mathrm{p}})}{\mathcal{B}(\mathrm{B}^+ \to \mathrm{K}^+\mathrm{J}/\psi) \times \mathcal{B}(\mathrm{J}/\psi \to \mathrm{p}\overline{\mathrm{p}})} < 0.008 \,@\, 95\%\ CL$
- $\frac{\mathcal{B}(\mathrm{B}^+ \to \mathrm{K}^+\mathrm{X}(3872)) \times \mathcal{B}(\mathrm{X}(3915) \to \mathrm{p}\overline{\mathrm{p}})}{\mathcal{B}(\mathrm{B}^+ \to \mathrm{K}^+\mathrm{J}/\psi) \times \mathcal{B}(\mathrm{J}/\psi \to \mathrm{p}\overline{\mathrm{p}})} < 0.032 \,@\, 95\%\ CL$

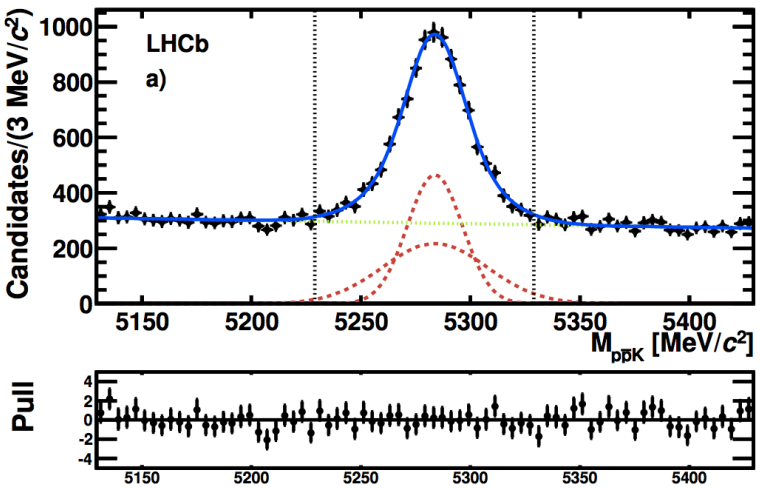

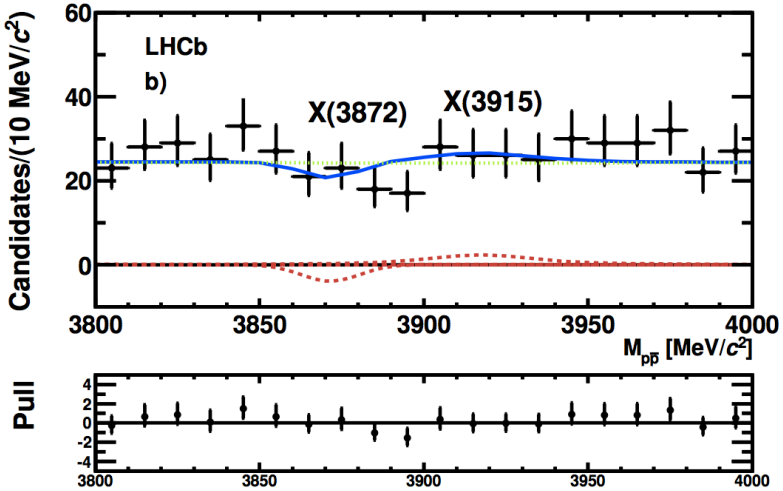

Evidence of $X(3872) \to \psi(2S)\gamma$

Nuclear Physics B 886 (2014) 665-680

Radiative decays of the $X(3872)$ provide a valuable opportunity to understand its nature.

- The $X(3872)$ C-parity has been determined studying the $X(3872) \to \gamma J/\psi$ decay.
- $R_{\psi\gamma} = \frac{\mathcal{B}(X(3872)\to\psi(2S)\gamma)}{\mathcal{B}(X(3872)\to J/\psi\,\gamma)}$ can give information about the internal structure of $X(3872)$.

- Analysis performed using 3 fb^{-1} collected in 2011 and 2012.
- Observed $4.4\,\sigma$ evidence of $X(3872) \to \psi(2S)\gamma$ in $B^+ \to K^+X(3872)$ decays.

Parameter		Decay mode $X(3872) \to J/\psi\gamma$	Decay mode $X(3872) \to \psi(2S)\gamma$
m_{B^+}	$[MeV/c^2]$	5277.7 ± 0.8	5281.9 ± 2.4
$m_{X(3872)}$	$[MeV/c^2]$	3873.4 ± 3.4	3869.5 ± 3.4
N_ψ		591 ± 48	36.4 ± 9.0

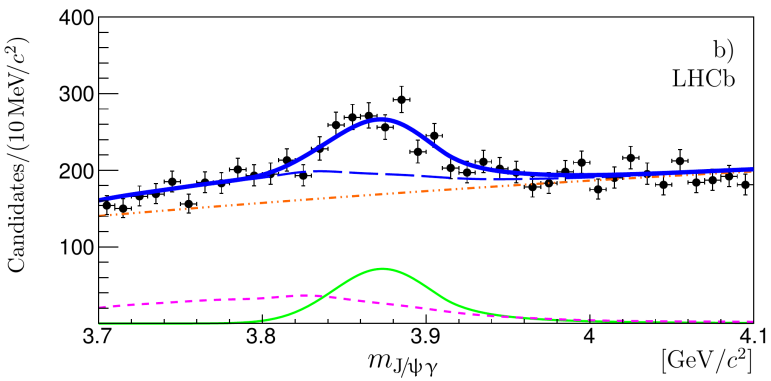

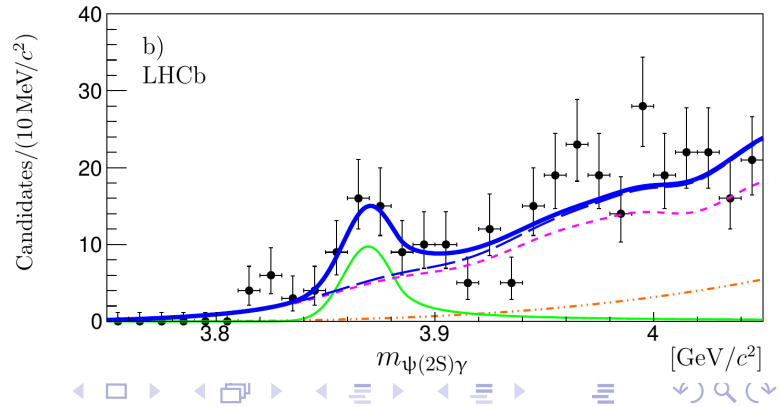

Evidence of $X(3872) \to \psi(2S)\gamma$

Nuclear Physics B 886 (2014) 665-680

- $$R_{\psi(2S)\gamma} = \frac{\mathcal{B}(X(3872) \to \psi(2S)\gamma)}{\mathcal{B}(X(3872) \to J/\psi\,\gamma)} = 2.46 \pm 0.64 \pm 0.29$$

- These results disfavours $D^{*0}\bar{D}^{0}$ molecule hypothesis

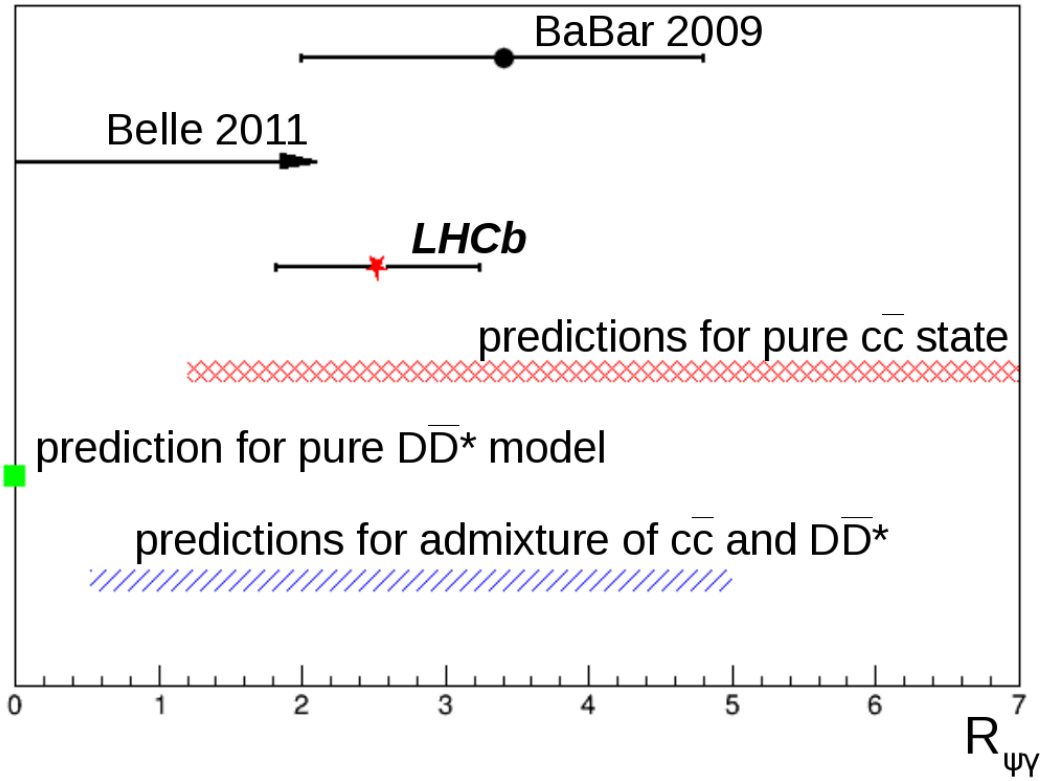

The X(4140) and X(4274) candidates

Two exotic resonance candidates observed by CDF in $B^{\pm} \to J/\psi\,\phi K^{\pm}$ decays and decaying into $J/\psi\,\phi$.

[Ref. Phys.Rev.Lett. 102.242002, arXiv:1101.6058].

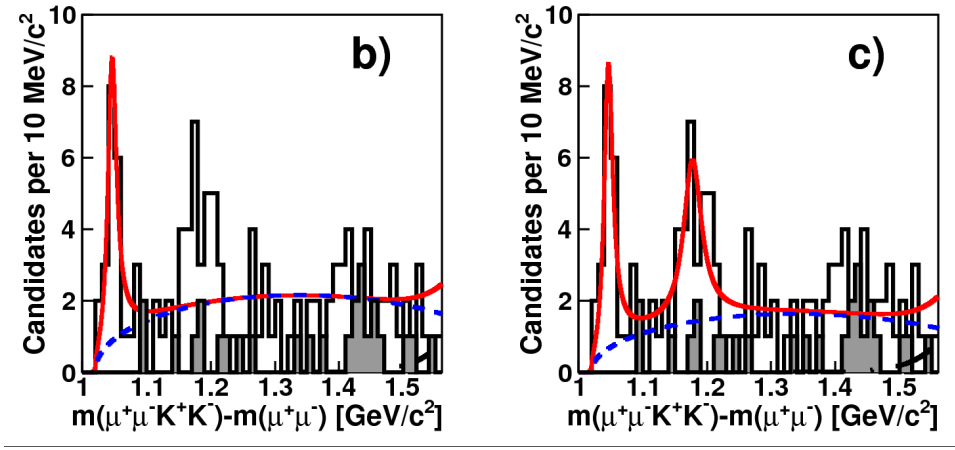

- 115 ± 12 candidates of $B^{\pm} \to J/\psi\,\phi K^{\pm}$
- $X(4140)$ candidate with $M_{X(4140)} = 4143.4^{+2.9}_{-3.0} \pm 0.6\ \mathrm{MeV}/c^2$, $\Gamma_{X(4140)} = 15.3^{+10.4}_{-6.1} \pm 2.5\ \mathrm{MeV}/c^2$, with yield of 19 ± 6 and statistical significance of 5.0σ.
- Maybe a second state: $M_{X(4274)} = 4274.4^{+8.4}_{-6.4} \pm 1.9\,\mathrm{MeV}/c^2$, $\Gamma_{X(4274)} = 32.3^{+21.9}_{-15.3} \pm 7.6\,\mathrm{MeV}/c^2$, with yield of 22 ± 8 and statistical significance of 3.1σ.
- CDF results imply:

$$\mathcal{B}(B^+ \to X(4140)K^+) \times \mathcal{B}(X(4140) \to J/\psi\,\phi) = (5.2 \pm 1.7) \times 10^{-5}$$

The X(4140) and X(4274) candidates

Belle experiment also have searched for X(4140) and X(4274)

[see J. Brodzicka, Heavy flavour spectroscopy (LP09)]

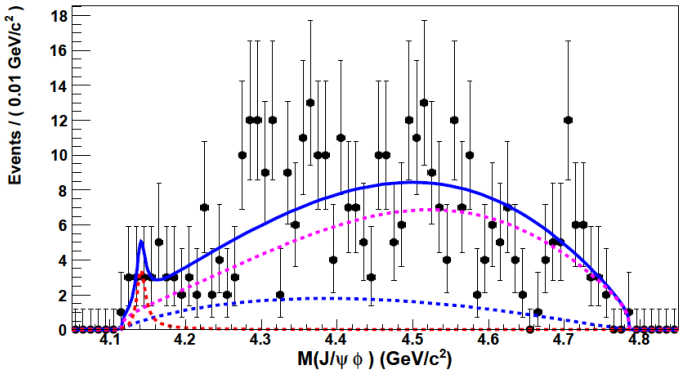

- Belle accumulated more events on $B^+ \to J/\psi\phi K^+$ than CDF but could not confirm or exclude the X(4140).
- Loss of efficiency near the threshold resulted in a lower sensitivity to X(4140) at Belle.
- $\mathcal{B}(B^+ \to X(4140)K^+) \times \mathcal{B}(X(4140) \to J/\psi\phi) < 6 \times 10^{-6}$

In summary:

- Charmonium states at this mass are expected to have much larger widths because of open flavour decay channels.
- Their decay rate into the $J/\psi\,\phi$ mode (so near the kinematic threshold) should be small and unobservable.
- Then, the observation by CDF has triggered much theoretical interest about the nature of this candidates.
- The existence of X(4140) and X(4274) candidates remains unconfirmed.

Search for $\mathrm{X}(4140)$ and $\mathrm{X}(4274)$

- The LHCb sensitivity to $\mathrm{X}(4140)$ signal is a factor two better than in CDF.
- According the CDF results, we should observe 35 ± 11 $\mathrm{X}(4140)$ signal candidates and 53 ± 19 $\mathrm{X}(4274)$ signal candidates.
- No narrow structure is observed near the threshold.
- The fit shown in (a) gives a $\mathrm{X}(4140)$ yield of 6.9 ± 4.9 events and a $\mathrm{X}(4274)$ yield of $3.4^{+6.5}_{-3.4}$ events.
- The fit shown in (b) gives a $\mathrm{X}(4140)$ yield of 0.6 events with a positive error of 7.1 events and zero signal $\mathrm{X}(4274)$ events with a positive error of 10.

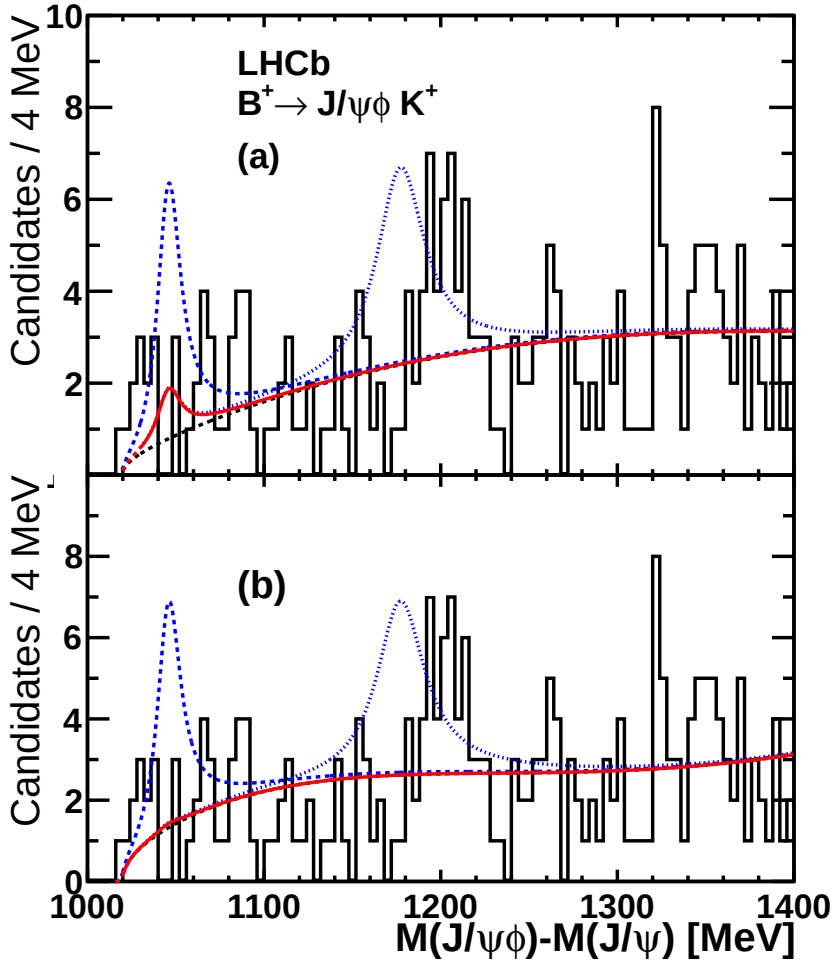

- The solid red line represents the result of the fit to our data.
- The dashed blue line represents the the expected signal amplitude from the CDF results.
- The top and bottom plots background functions are: a) efficiency-corrected three-body phase-space; b) quadratic polynominal.

Results on $\mathrm{X}(4140)$ and $\mathrm{X}(4274)$ at LHCb

Phys. Rev. D 85,091103(R)(2012)

The results of the search for $\mathrm{X}(4140)$ and $\mathrm{X}(4274)$ at LHCb are the two following limits calculated at 90%CL:

$$\frac{\mathcal{B}(\mathrm{B}^+ \to \mathrm{X}(4140)\mathrm{K}^+) \times \mathcal{B}(\mathrm{X}(4140) \to \mathrm{J}/\psi\phi)}{\mathcal{B}(\mathrm{B}^+ \to \mathrm{J}/\psi\phi\mathrm{K}^+)}$$

LHCb(a)	LHCb(b)	CDF
< 0.07	< 0.04	$0.149 \pm 0.039 \pm 0.024$

$$\frac{\mathcal{B}(\mathrm{B}^+ \to \mathrm{X}(4274)\mathrm{K}^+) \times \mathcal{B}(\mathrm{X}(4274) \to \mathrm{J}/\psi\phi)}{\mathcal{B}(\mathrm{B}^+ \to \mathrm{J}/\psi\phi\mathrm{K}^+)}$$

LHCb	CDF (our estimate)
< 0.08	0.17 ± 0.06

In conclusion, LHCb performed the most sensitive search for the narrow $\mathrm{X}(4140)$ and $\mathrm{X}(4274)$ structures and:

- Does not confirm the $\mathrm{X}(4140)$ state previously reported by the CDF
- Does not observe any evidence of the $\mathrm{X}(4274)$
- The LHCb results disagree at the 2.4σ level with the CDF measurement.

Backup: Miscellaneous

The LHCb trigger and dataset

Running conditions in most of 2012

- LHC: 20 MHz bunch crossing
- Luminosity: $4.0 \times 10^{32} cm^{-2} s^{-1}$, using luminosity leveling
- Visible interactions rate: 12.0 - 14.0 MHz
- L0 output rate: 950 kHz
- HLT output rate:4.5 kHz
- Event size: 60 kB

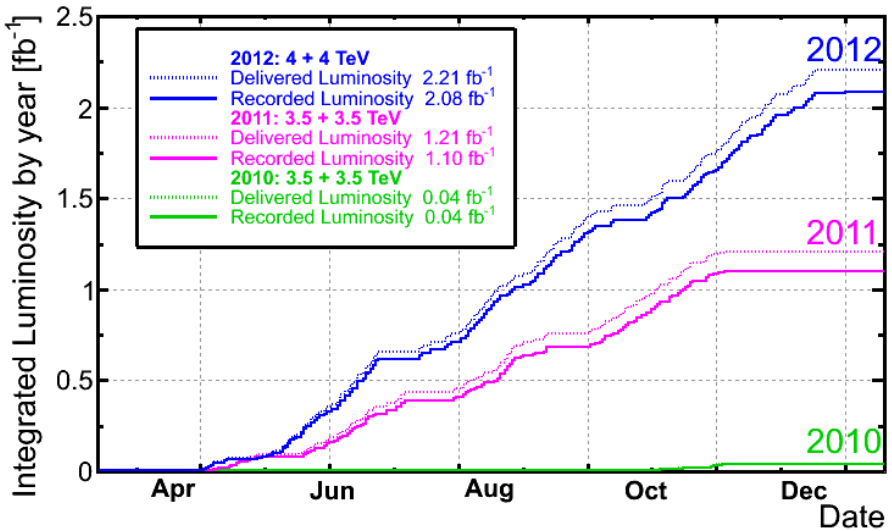

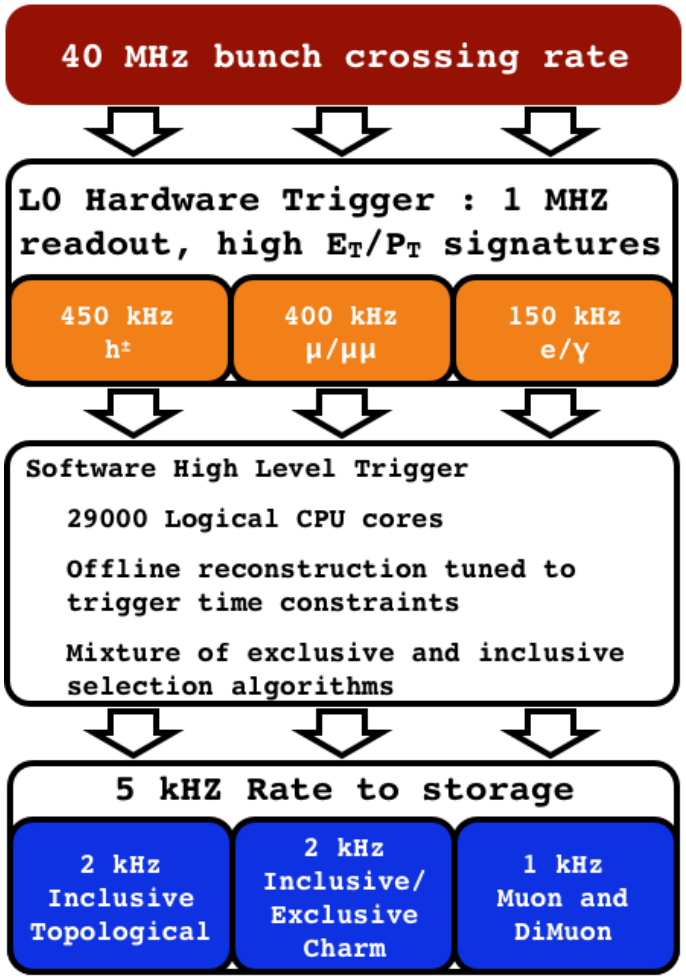

37 pb^{-1} **acquired in 2010**

1 fb^{-1} **acquired in 2011**

2 fb^{-1} **acquired in 2012**

X(3872) mass measurement at LHCb: uncertainties

Source of uncertainty	$\Delta\sigma/\sigma$ [%]
$X(3872)$ polarization	2.1
$X(3872)$ decay model	1.0
$X(3872)$ decay width	5.0
Mass resolution	5.8
Background model	6.4
Tracking efficiency	7.4
Track χ^2 cut	2.0
Vertex χ^2 cut	3.0
Muon trigger efficiency	2.9
Global event cuts	3.0
Muon identification	1.1
Integrated luminosity	3.5
$J/\psi \to \mu^+\mu^-$ branching fraction	1.0
Total	14.3

Category	Source of uncertainty	Δm [MeV/c^2]	
		$\psi(2S)$	$X(3872$
Mass fitting	Natural width	–	0.01
	Radiative tail	0.02	0.02
	Resolution	–	0.01
	Background model	0.02	0.02
Momentum calibration	Average momentum scale	0.08	0.10
	η dependence of momentum scale	0.02	0.03
Detector description	Energy loss correction	0.05	0.05
Detector alignment	Track slopes	0.01	0.01
Total		0.10	0.12

Search for $\mathrm{X}(4140)$ and $\mathrm{X}(4274)$ at LHCb

- LHCb searched for $\mathrm{X}(4140)$ and $\mathrm{X}(4274)$ in a sample with 0.376 fb^{-1} of 2011 dataset [Ref. Phys. Rev. D 85, 091103(R) (2012)].
- Background subtracted sample with 382 ± 22 $\mathrm{B}^{\pm} \to \mathrm{J}/\psi\,\phi\mathrm{K}^{\pm}$ events

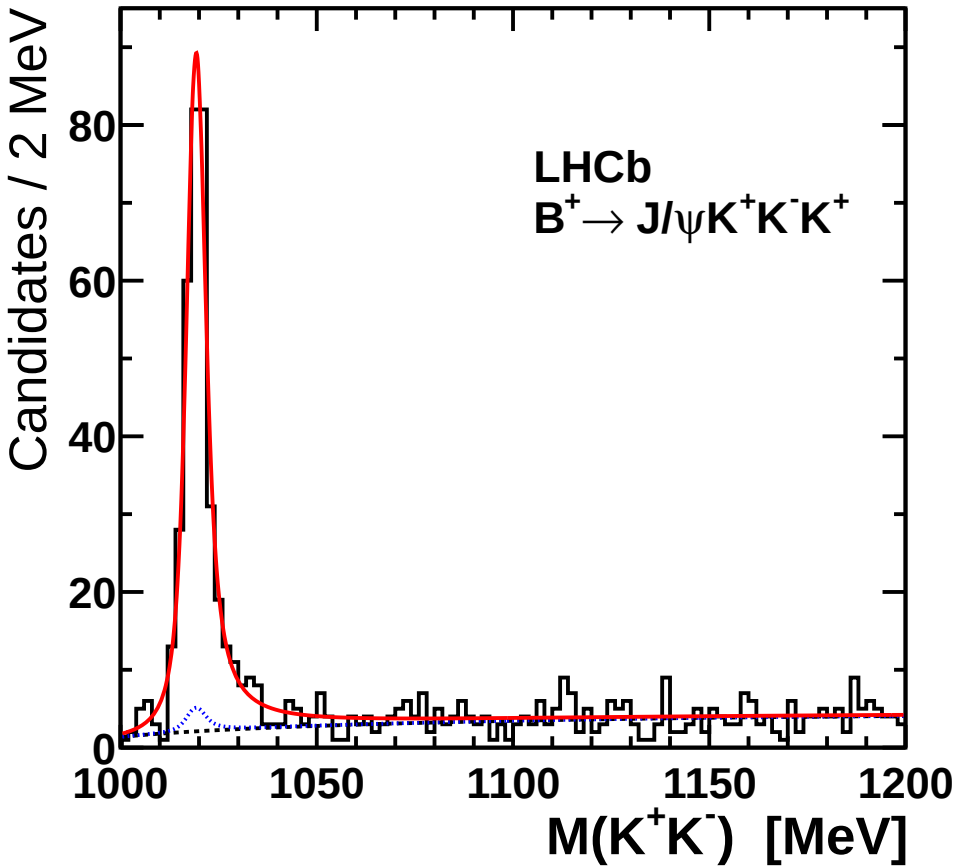

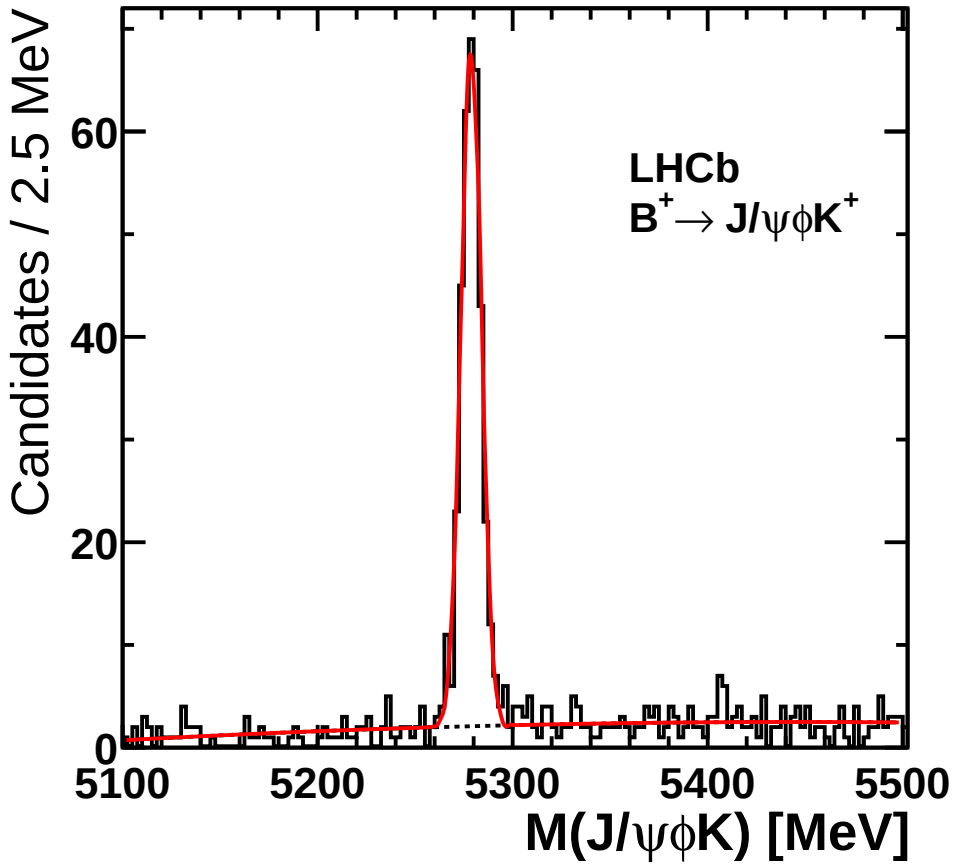

Search for X(4140) and X(4274) at LHCb:efficiency

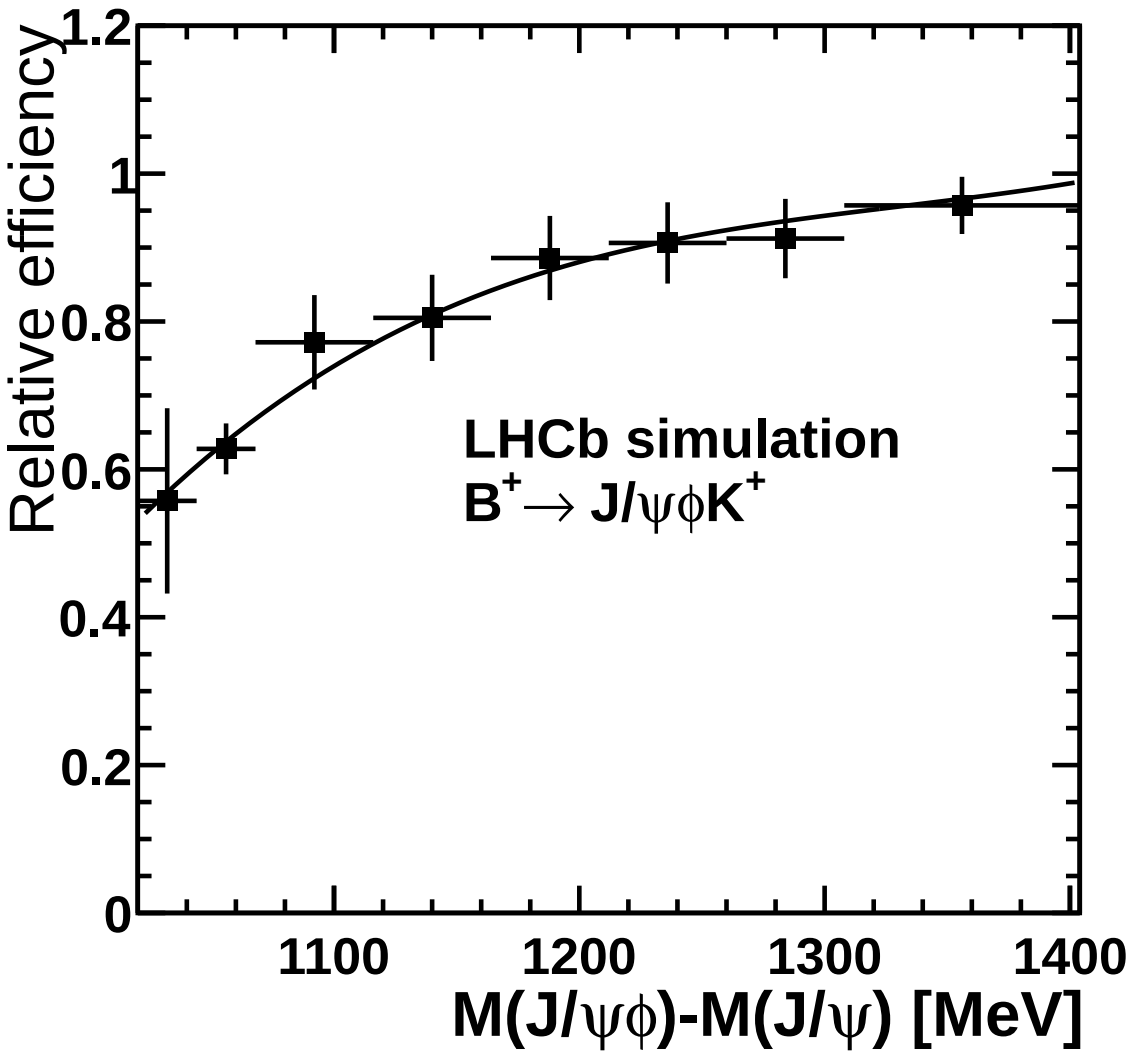

$\mathrm{X}(3872)$ quantum numbers: previous measurements

CDF

- Sample dominated by prompt $\mathrm{X}(3872)$
- 3D analysis: fit to $\pi^+\pi^-$ and J/ψ helicity angles and te angle between the $\pi^+\pi^-$ and J/ψ decay planes
- $\mathrm{X}(3872)$ J^{PC} constrained to 1^{++} or 2^{-+}
- Phys.Rev.Lett.98:132002 (2007)

BaBar

- Observed 34 ± 7 $\mathrm{X}(3872) \to \omega \mathrm{J}/\psi$
- Study of $\omega \to \pi^-\pi^+\pi^0$ mass distribution favoured 2^{-+}, but 1^{++} was not ruled out.
- arXiv:1005.5190, Phys. Rev. D 82, 011101(R) (2010)

Belle

- Observed 173 ± 16 $\mathrm{B} \to \mathrm{X}(3872)\mathrm{K}$, with $\mathrm{X}(3872) \to \mathrm{J}/\psi\pi^+\pi^-$ and $\mathrm{J}/\psi \to \mu^+\mu^-$
- By studying one-dimensional distributions in three different angles, Belle concluded that their data were equally well described by the 1^{++} and 2^{-+} hypotheses.
- arXiv:1107.0163, Phys. Rev. D 84, 052004 (2011)

X(3872) production studies at CMS

CMS collaboration performed detailed X(3872) production studies using the decay mode $X(3872) \to J/\psi \pi^+\pi^-$, with $J/\psi \to \mu^+\mu^-$ and 4.1 fb^{-1} 7 TeV

- Measurements are performed in the range $10 < p_{T\,X(3872)} < 50$ GeV and rapidity $|y| < 1.2$.
- Detailed study of the dipion mass showing the decay proceeds dominantly through a intermediate ρ

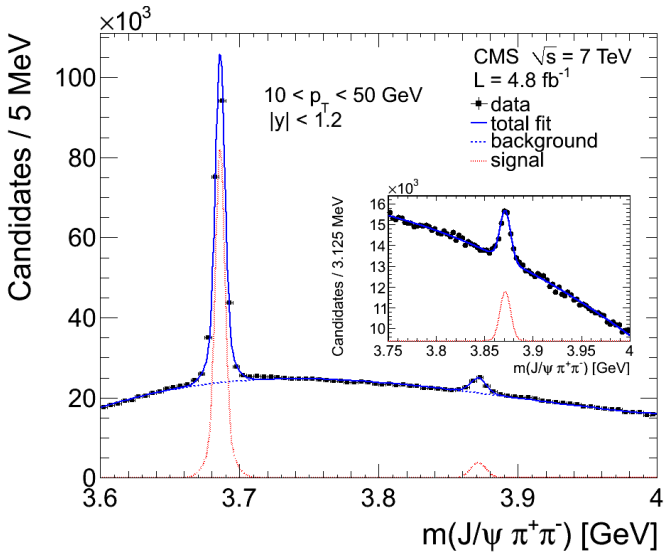

[arXiv:1302.3968]

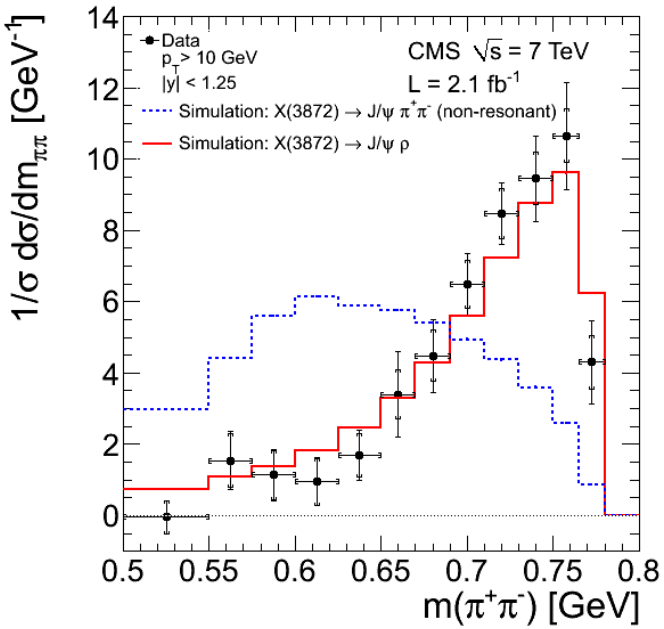

X(3872) production studies at CMS

- Ratio of the X(3872) and $\psi(2S)$ cross sections times their branching fractions into $J/\psi\pi^+\pi^-$ measured in function of p_T.
- Fraction of X(3872) originating from B decays.
- Prompt X(3872) differential cross section times branching fraction into $J/\psi\pi^+\pi^-$ and comparison with theory prediction.

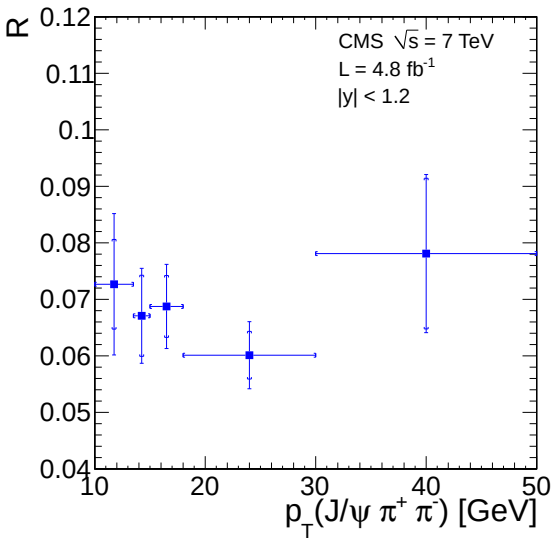

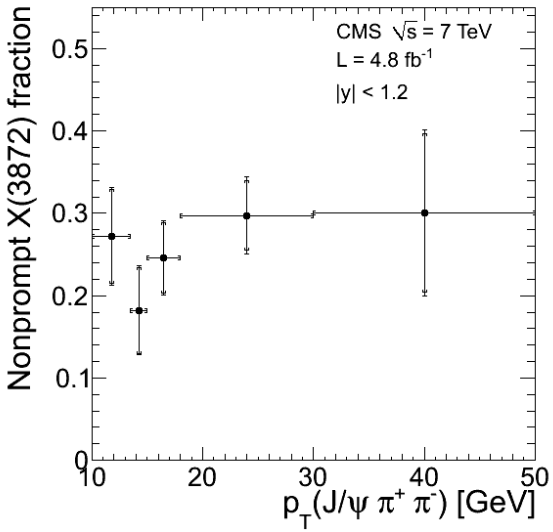

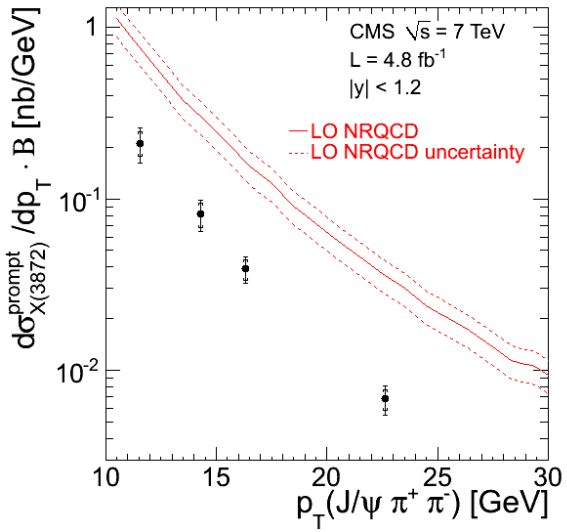

[arXiv:1302.3968]

$J/\psi\ \pi^+$ mass in $B^0 \to J/\psi \pi^+\pi^-$

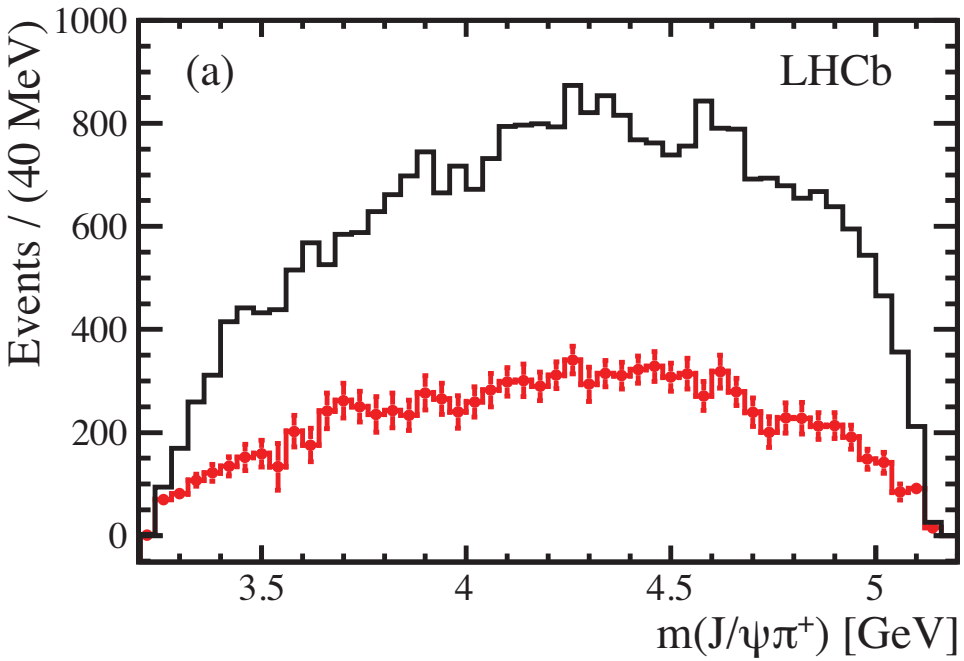

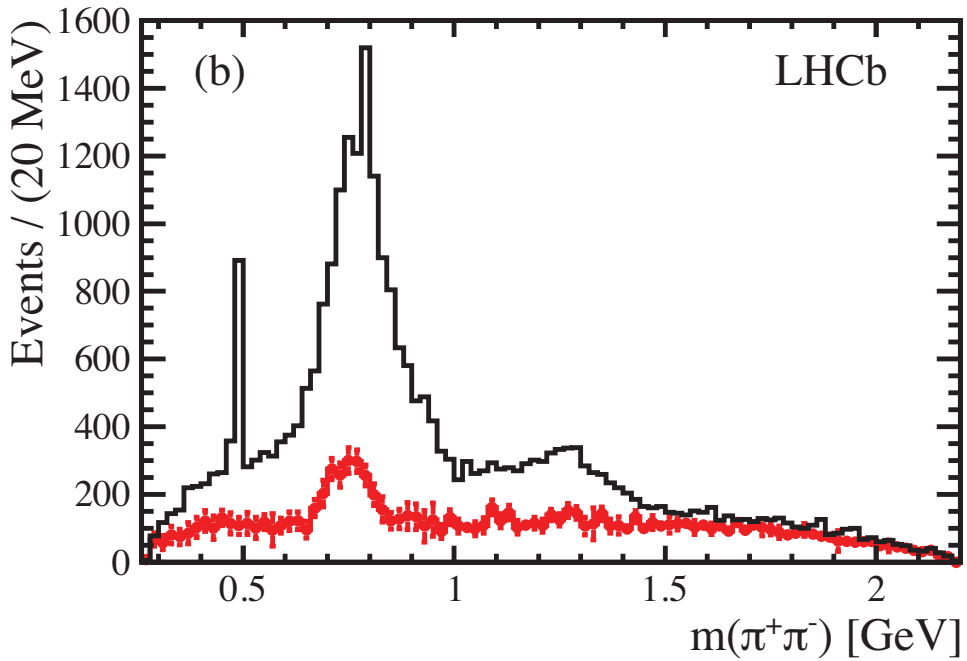

Spectroscopy in light quark sector: $\mathrm{B}^0 \to \mathrm{J}/\psi\,\pi^+\pi^-$

Phys. Rev. D 87, 052001

- The substructure of mesons belonging to the scalar nonet is controversial.
- Many possibilities: $\mathrm{q\bar{q}}$, $\mathrm{q\bar{q}q\bar{q}}$, mixtures etc.
- $\mathrm{q\bar{q}}$ case:

$$\begin{aligned} |f_0(980)\rangle &= \cos\varphi_m |s\bar{s}\rangle + \sin\varphi_m |n\bar{n}\rangle \\ |f_0(500)\rangle &= -\sin\varphi_m |s\bar{s}\rangle + \cos\varphi_m |n\bar{n}\rangle, \\ \text{where } |n\bar{n}\rangle &\equiv \frac{1}{\sqrt{2}}\left(|u\bar{u}\rangle + |d\bar{d}\rangle\right). \end{aligned}$$

- $\mathrm{q\bar{q}q\bar{q}}$ case:

$$\begin{aligned} |f_0(980)\rangle &= \frac{1}{\sqrt{2}}\left(|[su][\bar{s}\,\bar{u}]\rangle + |[sd][\bar{s}\bar{d}]\rangle\right) \\ |f_0(500)\rangle &= |[ud][\bar{u}\bar{d}]\rangle. \end{aligned}$$

- Observable of interest for both cases:

$$\tan^2\varphi_m \equiv r_\sigma^f = \frac{\mathcal{B}\left(\overline{B}^0 \to J/\psi\, f_0(980)\right)}{\mathcal{B}\left(\overline{B}^0 \to J/\psi\, f_0(500)\right)} \frac{\Phi(500)}{\Phi(980)}$$

- Prediction for tetraquark states: $r_\sigma^f = 1/2$ [PRL 111, 062001 (2013)]

Amplitude analysis of $B^0 \to J/\psi \pi^+\pi^-$

Phys. Rev. D 87, 052001

- Approach similar to the $Z(4430)^+$ analysis: 4D matrix element describing π^+ π^- resonances;
- No evidence of $J/\psi \pi^+$ resonances
- 19,000 B^0 signal candidates
- Background modelled from sidebands

Signal B^0 candidates in red.

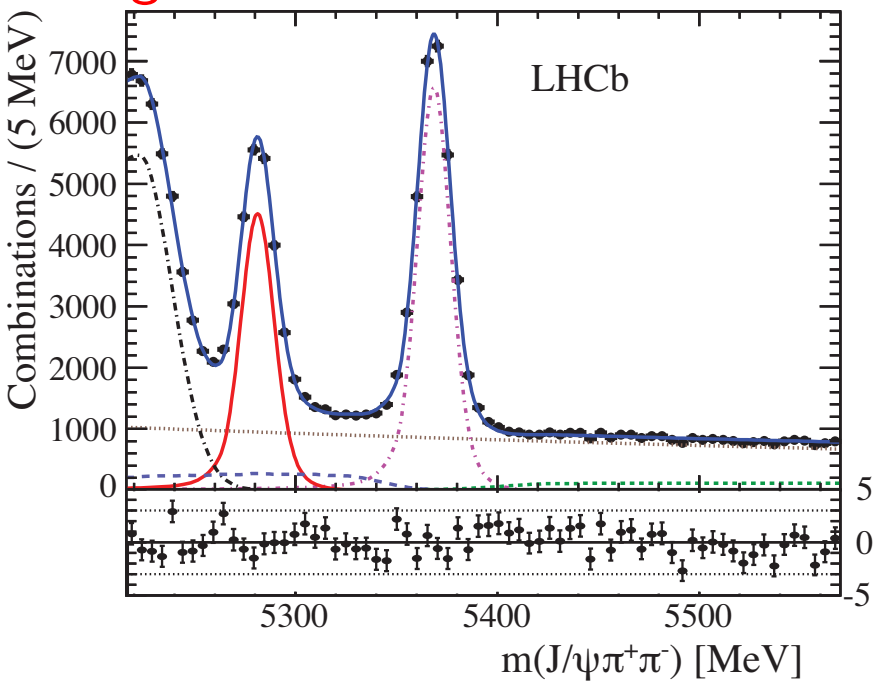

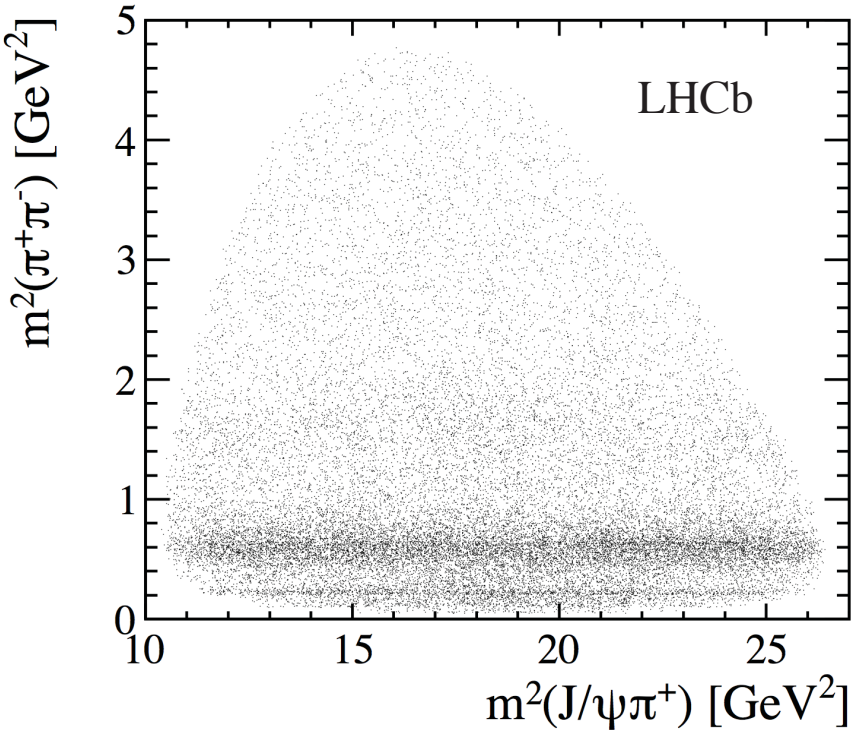

Amplitude analysis of $B^0 \to J/\psi \pi^+\pi^-$

Phys. Rev. D 87, 052001

R	$\mathcal{B}(\overline{B}^0 \to J/\psi R, R \to \pi^+\pi^-)$
$\rho(770)$	$(2.50 \pm 0.10^{+0.18}_{-0.15}) \times 10^{-5}$
$f_0(500)$	$(8.8 \pm 0.5^{+1.1}_{-1.5}) \times 10^{-6}$
$f_2(1270)$	$(3.0 \pm 0.3^{+0.2}_{-0.3}) \times 10^{-6}$
$\omega(782)$	$(2.7^{+0.8+0.7}_{-0.6-0.5}) \times 10^{-7}$
$\rho(1450)$	$(4.6 \pm 1.1 \pm 1.9) \times 10^{-6}$
$\rho(1700)$	$(2.0 \pm 0.5 \pm 1.2) \times 10^{-6}$

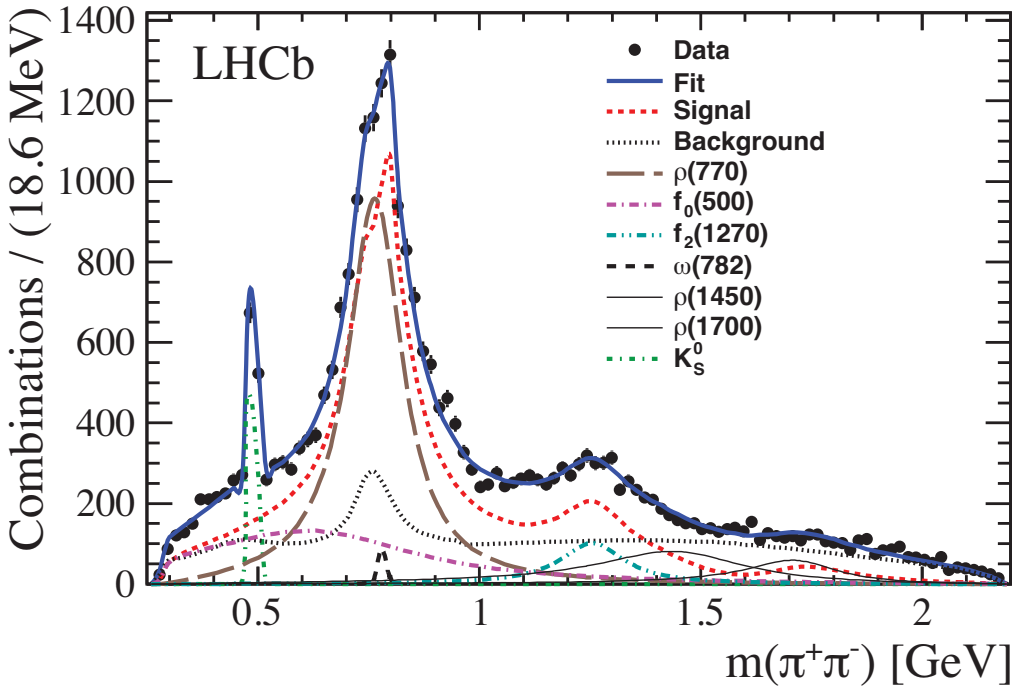

- Best fit model shows does not require $f_0(980)$ component.
- Upper limit on the $f_0(500) - f_0(980)$ mixing angle.
- Different from tetraquark prediction (1/2) by 8σ

$$\tan^2 \varphi_m \equiv r_\sigma^f = \left(1.1^{+1.2+6.0}_{-0.7-0.7}\right) \times 10^{-2} < 0.098 \quad \text{at } 90\% \text{ C.L}$$